

Dynamic critical exponent of two-, three-, and four-dimensional XY models with relaxational and resistively shunted junction dynamics

Lars Melwyn Jensen, Beom Jun Kim, and Petter Minnhagen
Department of Theoretical Physics, Umeå University, 901 87 Umeå, Sweden

The dynamic critical exponent z is determined numerically for the d -dimensional XY model ($d = 2, 3$, and 4) subject to relaxational dynamics and resistively shunted junction dynamics. We investigate both the equilibrium fluctuation and the relaxation behavior from nonequilibrium towards equilibrium, using the finite-size scaling method. The resulting values of z are shown to depend on the boundary conditions used, the periodic boundary condition, and fluctuating twist boundary condition (FTBC), which implies that the different treatments of the boundary in some cases give rise to different critical dynamics. It is also found that the equilibrium scaling and the approach to equilibrium scaling for the the same boundary condition do not always give the same value of z . The FTBC in conjunction with the finite-size scaling of the linear resistance for both type of dynamics yields values of z consistent with expectations for superfluids and superconductors: $z = 2, 3/2$, and 2 for $d = 2, 3$, and 4 , respectively.

PACS numbers: 74.40.+k, 05.70.Jk, 75.40.Gb, 75.40.Mg

I. INTRODUCTION

Superconducting films, Josephson junction arrays, and superfluid ^4He are systems where topological defects play an important role close to the phase transition. This is particularly striking in two dimensions (2D) where a phase transition of the Kosterlitz-Thouless (KT) nature is driven by the unbinding of thermally created topological defects, vortex-antivortex pairs.^{1,2} In 3D such topological defects take the form of vortex loops and it has been argued that the physics close to the transition can be associated with these loops.³ The common feature in these systems is that they can be characterized by a complex order parameter. The XY model can be viewed as a discretized version of such systems where only the phase of the complex order parameter plays a significant role. This model is believed to catch the essential features of the topological defects present in ^4He as well as in superconductors in the limit when the magnetic penetration length is much larger than the correlation length; high- T_c superconductors fall into this category.⁴ All the systems which can be described by the XY model belong to the same universality class for the thermodynamic critical properties of the phase transition.

In the present paper we have the connection between the XY model and superfluid and superconducting systems in mind. However, the XY model *per se* can equally well be viewed as a simple model of a ferromagnet where the phase angle corresponds to the direction of a 2D spin vector associated with each lattice site.

Our interest in the present paper is the dynamical properties associated with topological defects, which may of course depend on the explicit choice of the dynamics imposed on the model. We here investigate two types of dynamics: One is a simple relaxational dynamics (RD) and the other is the resistively shunted junction dynamics (RSJD). We calculate the dynamic critical exponent z

using various scaling relations both associated with equilibrium and with the approach to equilibrium when starting from a nonequilibrium configuration. Our main conclusion is that the dynamic critical exponents associated with the topological defects are the same for these two types of dynamics, RD and RSJD. However, this conclusion does depend on the precise treatment of the boundary. We demonstrate that various values of z can be obtained by changing the treatment of the boundary, as well as by changing from scaling in equilibrium to scaling for the approach to equilibrium.

This paper is organized as follows: In Sec. II we briefly introduce the XY model and explain how the dynamic equations are defined in RSJD and RD taking boundary conditions into account. Section III describes the various scaling relations used to obtain z . The results from our simulations are given in Sec. IV for spatial dimensions $d = 2, 3$, and 4 , whereas Sec. V contains discussions of the results. Finally Sec. VI gives a short summary of the main conclusions.

II. XY MODEL AND DYNAMICS

A. XY model

The d -dimensional XY Hamiltonian on a hypercubic lattice of the size $\Omega \equiv L^d$ is defined by

$$H[\theta_{\mathbf{r}}] = -J \sum_{\langle \mathbf{r}\mathbf{r}' \rangle} \cos(\phi_{\mathbf{r}\mathbf{r}'} \equiv \theta_{\mathbf{r}} - \theta_{\mathbf{r}'}), \quad (1)$$

where the summation is over nearest neighboring pairs, $\theta_{\mathbf{r}}$ is the phase of the complex order parameter at position \mathbf{r} , and J is the coupling strength. The XY Hamiltonian is appropriate not only to describe the overdamped Josephson junctions arrays without charging energy, but

can also be viewed as a discretized form of the Ginzburg-Landau (GL) free energy

$$F_{GL}[\psi(\mathbf{r})] = \int d\mathbf{r} \left(\alpha |\psi(\mathbf{r})|^2 + \frac{\beta}{2} |\psi(\mathbf{r})|^2 + \frac{1}{2} |\nabla\psi(\mathbf{r})|^2 \right), \quad (2)$$

where the amplitude fluctuations of the complex order parameter $\psi(\mathbf{r})$ are neglected: $\psi(\mathbf{r}) = \psi_0 e^{i\theta(\mathbf{r})}$ with ψ_0 fixed to a constant. When mapping the GL free energy functional onto the XY Hamiltonian the coupling strength J is found to be proportional to $|\psi_0|^2$.

The thermodynamic properties of the XY model have been intensely studied for many years and it is well known that the important length scale in the critical region, the correlation length ξ , diverges at the critical temperature T_c . In 3D and 4D the divergence is of the standard form of the continuous second-order transition, i.e., $\xi(T) \sim |T - T_c|^{-\nu}$, whereas in 2D $\ln \xi(T) \sim (T - T_c)^{-1/2}$ as T_c is approached from above and $\xi = \infty$ in the whole low-temperature phase where quasi-long-range order exists in the absence of true long-range order.¹ From the point of view of the finite-size scaling, this feature of the 2D KT transition turns the finite system size L into the relevant length scale in the low-temperature phase.

B. Boundary condition

Experiments on superconductors and ⁴He are usually done on samples with open boundaries. From this perspective it is preferable to use boundary conditions, which reflects this experimental situation also in the simulations. However, simulations of the XY model can usually only be well converged on relatively small lattice sizes, and since the surface to volume ratio is inversely proportional to the linear system size L , the open boundary gives rise to large surface effects, which decay very slowly as the system size is increased. The standard way of reducing these unwanted surface effects is to impose the periodic boundary condition (PBC): $\theta_{\mathbf{r}+L\hat{\mu}} = \theta_{\mathbf{r}}$, where $\hat{\mu}$ denotes the basis vectors of the lattice, e.g., $\hat{\mu} = \hat{x}, \hat{y}, \hat{z}$ in 3D. One drawback of this boundary condition is that it restricts the twist from \mathbf{r} to $\mathbf{r} + L\hat{\mu}$, defined as the sum of the phase differences along a direct path connecting the two positions, to an integer multiple of 2π . On the other hand, this twist from one boundary to the opposite for an open system can have any value. It is thus preferable to relax the PBC so as to allow for a continuous twist by changing the boundary condition to a more generalized form: $\theta_{\mathbf{r}+L\hat{\mu}} = \theta_{\mathbf{r}} + L\Delta_{\mu}$, which has been used in various contexts.⁵⁻⁸ In particular the boundary condition where the twist variable Δ_{μ} is not fixed to a constant but allowed to fluctuate has been termed the fluctuating twist boundary condition (FTBC), which was originally introduced for static Monte Carlo (MC) simulations⁷ and then extended to Langevin-type dynamics

at finite temperatures.⁸ Since the FTBC allows for any value of the twist, it is closer to the open boundary condition for a real system. Of course one does not expect the treatment of the boundary to affect the results in the thermodynamic limit. However, as we will show and discuss here, the dynamics at criticality can depend on the boundary condition, in as far as the dynamic critical exponent can be defined in terms of the finite-size scaling. It is worth mentioning that a similar observation, i.e., that an important exponent may depend on boundary conditions, has been made recently in the study of the stiffness exponent of vortex-glass models.⁹

C. Dynamic models

Next we introduce two simple dynamic models widely used to describe behaviors of superfluids, superconducting films, regular Josephson junction arrays, and also bulk high T_c superconductors close to the transition temperature.

1. Resistively shunted junction dynamics

A d -dimensional hypercubic array of size $\Omega = L^d$ ($L =$ linear size) of superconducting grains weakly coupled by resistively shunted Josephson junctions is effectively described by the XY Hamiltonian (1) when it comes to the static properties. On the other hand, dynamic equations of motion for the corresponding overdamped RSJ model are generated from local conservation of the current on each grain. The total current $I_{\mathbf{r}\mathbf{r}'}$ between neighboring grains (\mathbf{r}, \mathbf{r}') is the sum of the supercurrent, the normal resistive current, and the thermal noise current: $I_{\mathbf{r}\mathbf{r}'} = I_{\mathbf{r}\mathbf{r}'}^s + I_{\mathbf{r}\mathbf{r}'}^n + I_{\mathbf{r}\mathbf{r}'}^t$. The supercurrent is given by the Josephson current-phase relation $I_{\mathbf{r}\mathbf{r}'}^s = I_c \sin(\phi_{\mathbf{r}\mathbf{r}'})$, where $I_c = 2eJ/\hbar$ is the critical current for a single junction. The normal resistive current $I_{\mathbf{r}\mathbf{r}'}^n = V_{\mathbf{r}\mathbf{r}'}/R_0$, where the voltage difference $V_{\mathbf{r}\mathbf{r}'}$ is related to the phase difference by $V_{\mathbf{r}\mathbf{r}'} = (\hbar/2e)\dot{\phi}_{\mathbf{r}\mathbf{r}'}$ and R_0 is the shunt resistance. Finally the thermal noise currents $I_{\mathbf{r}\mathbf{r}'}^t$ in the shunts satisfy $\langle I_{\mathbf{r}\mathbf{r}'}^t \rangle = 0$ and

$$\langle I_{\mathbf{r}_1\mathbf{r}_2}^t(t) I_{\mathbf{r}_3\mathbf{r}_4}^t(0) \rangle = \frac{2k_B T}{R_0} \delta(t) (\delta_{\mathbf{r}_1\mathbf{r}_3} \delta_{\mathbf{r}_2\mathbf{r}_4} - \delta_{\mathbf{r}_1\mathbf{r}_4} \delta_{\mathbf{r}_2\mathbf{r}_3}), \quad (3)$$

where $\langle \dots \rangle$ is the thermal average, and $\delta(t)$ and $\delta_{\mathbf{r}\mathbf{r}'}$ are the Dirac and Kronecker deltas, respectively. From local current conservation we obtain

$$\sum_{\hat{n}} I_{\mathbf{r}\mathbf{r}+\hat{n}} = I_{\mathbf{r}}^{\text{ext}}, \quad (4)$$

where the \hat{n} summation is over $2d$ nearest neighbors of site \mathbf{r} on a hypercubic lattice in d dimensions ($\hat{n} = \pm\hat{\mu}$), e.g., $\hat{n} = \pm\hat{x}, \pm\hat{y}, \pm\hat{z}$ in 3D, and $I_{\mathbf{r}}^{\text{ext}}$ is an external current source at \mathbf{r} (in the present work, we only consider

the case without external driving: $I_{\mathbf{r}}^{\text{ext}} = 0$). Introducing the lattice Green's function $U_{\mathbf{r}\mathbf{r}'}$, which is the inverse of the discrete Laplacian, the RSJD equations of motion in the absence of external currents can be written in dimensionless form as

$$\frac{d\theta_{\mathbf{r}}}{dt} = - \sum_{\mathbf{r}'} \bar{U}_{\mathbf{r}\mathbf{r}'} \sum_{\hat{n}} \sin(\theta_{\mathbf{r}'} - \theta_{\mathbf{r}'+\hat{n}}) + \zeta_{\mathbf{r}}, \quad (5)$$

where $\bar{U}_{\mathbf{r}\mathbf{r}'} \equiv U_{\mathbf{r}\mathbf{r}'} - U_{\mathbf{r}\mathbf{r}}$,¹⁰ and from here on we normalize the time, the current, the distance, the energy, and the temperature in units of $\hbar/2eR_0I_c$, I_c , the lattice spacing a , J , and J/k_B , respectively. The on-site noise term $\zeta_{\mathbf{r}}(t) \equiv -\sum_{\mathbf{r}'} \bar{U}_{\mathbf{r}\mathbf{r}'} \sum_{\hat{n}} I_{\mathbf{r}\mathbf{r}'+\hat{n}}^t(t)$ is spatially correlated, which is a consequence of the local current conservation, and satisfies $\langle \zeta_{\mathbf{r}}(t)\zeta_{\mathbf{r}'}(0) \rangle = 2T\bar{U}_{\mathbf{r}\mathbf{r}'}\delta(t)$. The RSJD equations (5) can be rewritten in a Langevin-type form¹⁰

$$\frac{d\theta_{\mathbf{r}}}{dt} = - \sum_{\mathbf{r}'} \bar{U}_{\mathbf{r}\mathbf{r}'} \frac{\delta H[\theta_{\mathbf{r}}]}{\delta \theta_{\mathbf{r}'}(t)} + \zeta_{\mathbf{r}}, \quad (6)$$

with the XY Hamiltonian H in Eq. (1) [compare with Eq. (12) for relaxational dynamics].

We now introduce the FTBC for the RSJD. The global twist $L\Delta_{\mu}$ in the $\hat{\mu}$ direction across the whole system (see Sec. II B) is introduced through the local transformation $\theta_{\mathbf{r}} \rightarrow \theta_{\mathbf{r}} + \mathbf{r} \cdot \Delta$, still keeping $\theta_{\mathbf{r}} = \theta_{\mathbf{r}+L\hat{\mu}}$ as the periodic part of the phases. The Hamiltonian in terms of these variables is

$$H[\theta_{\mathbf{r}}, \Delta] = - \sum_{\mathbf{r}\hat{\mu}} \cos(\theta_{\mathbf{r}} - \theta_{\mathbf{r}+\hat{\mu}} - \hat{\mu} \cdot \Delta), \quad (7)$$

where the $\hat{\mu}$ summation is over d nearest neighbors of \mathbf{r} in each positive direction (e.g., $\hat{\mu} = \hat{x}, \hat{y}, \hat{z}$ in 3D). It is straightforward to show that equations of motion for phase variable $\theta_{\mathbf{r}}$ are given by Eq. (6) with the substitution H given by Eq. (7):⁸

$$\frac{d\theta_{\mathbf{r}}}{dt} = - \sum_{\mathbf{r}'} \bar{U}_{\mathbf{r}\mathbf{r}'} \frac{\delta H[\theta_{\mathbf{r}}, \Delta]}{\delta \theta_{\mathbf{r}'}(t)} + \zeta_{\mathbf{r}}. \quad (8)$$

In order to get a closed set of equations we further have to specify the dynamics of the twist variables Δ_{μ} , which is simply the average phase difference between opposite faces on the d -dimensional hypercube. In the absence of external currents, the physical boundary condition, corresponding to an open boundary in real systems, should satisfy the condition that there be no current across the boundary, which leads to⁸

$$\frac{d\Delta_{\mu}}{dt} = \Gamma_{\Delta} \sum_{\mathbf{r}} \sin(\theta_{\mathbf{r}} - \theta_{\mathbf{r}+\hat{\mu}} - \Delta_{\mu}) + \zeta_{\mu}^{\Delta} \quad (9)$$

or, equivalently,

$$\frac{d\Delta_{\mu}}{dt} = -\Gamma_{\Delta} \frac{\delta H[\theta_{\mathbf{r}}, \Delta]}{\delta \Delta_{\mu}} + \zeta_{\mu}^{\Delta}, \quad (10)$$

where $\Gamma_{\Delta} = 1/L^d$. As shown in Ref. 8 the noise term satisfies $\langle \zeta_{\mu}^{\Delta}(t) \rangle = \langle \zeta_{\mu}^{\Delta}(t)\zeta_{\mathbf{r}}(t') \rangle = 0$ and $\langle \zeta_{\mu}^{\Delta}(t)\zeta_{\nu}^{\Delta}(0) \rangle = 2T\Gamma_{\Delta}\delta_{\mu\nu}\delta(t)$. We term the dynamics defined in this way [by Eqs. (8) and (10)] RSJD with the FTBC, whereas the RSJD with the PBC is given by Eq. (6) with H in Eq. (1).

2. Relaxational dynamics

Next we introduce the simpler phenomenological relaxational dynamics called time-dependent Ginzburg-Landau-Langevin dynamics, which represents a nonconserved dynamics,¹¹ for the complex order parameter $\psi_{\mathbf{r}}$ on a discrete lattice:

$$\frac{d\psi_{\mathbf{r}}}{dt} = -\Gamma \frac{\delta F_{GL}[\psi_{\mathbf{r}}]}{\delta \psi_{\mathbf{r}}(t)} + \zeta_{\mathbf{r}}, \quad (11)$$

where Γ is the diffusion constant, F_{GL} is the discrete version of the GL free energy functional (2), and the white noise term satisfies $\langle \zeta_{\mathbf{r}}(t) \rangle = 0$ and $\langle \zeta_{\mathbf{r}}(t)\zeta_{\mathbf{r}'}(0) \rangle = 2k_B T \Gamma \delta_{\mathbf{r}\mathbf{r}'} \delta(t)$. The order parameter relaxes towards a configuration which locally minimizes the free energy, and the noises force the metastable states to decay. In the London limit the system can be described solely by the phase $\theta_{\mathbf{r}}(t)$ of the order parameter $\psi_{\mathbf{r}} = \psi_0 e^{i\theta_{\mathbf{r}}}$ with ψ_0 fixed to a constant. Hence, by neglecting the amplitude fluctuations and discretizing the time-dependent Ginzburg-Landau equation of motion, we find the phase equations of motion for the RD defined by

$$\frac{d\theta_{\mathbf{r}}}{dt} = - \frac{\delta H[\theta_{\mathbf{r}}]}{\delta \theta_{\mathbf{r}}(t)} + \zeta_{\mathbf{r}}, \quad (12)$$

where H is the XY Hamiltonian (1) in units of J , the time unit is $\hbar/\Gamma J$, and the dimensionless thermal noises satisfy $\langle \zeta_{\mathbf{r}}(t) \rangle = 0$ and

$$\langle \zeta_{\mathbf{r}}(t)\zeta_{\mathbf{r}'}(0) \rangle = 2T\delta(t)\delta_{\mathbf{r}\mathbf{r}'}, \quad (13)$$

with T in units of J/k_B . From Eq. (12), the RD equations for the phases in the case of the PBC are given by

$$\frac{d\theta_{\mathbf{r}}}{dt} = - \sum_{\mathbf{r}\hat{n}} \sin(\theta_{\mathbf{r}} - \theta_{\mathbf{r}+\hat{n}}) + \zeta_{\mathbf{r}}, \quad (14)$$

with periodicity on the phase variables: $\theta_{\mathbf{r}} = \theta_{\mathbf{r}+L\hat{\mu}}$.

We now proceed to the case of the FTBC for RD. In this case, in addition to the equations of motion for phases (Eq. (12) with substitution $H[\theta_{\mathbf{r}}]$ by $H[\theta_{\mathbf{r}}, \Delta]$ in Eq. (7)) we need dynamic equations for the twist variables Δ_{μ} . Relaxational dynamics means that these equations are of the form

$$\frac{d\Delta_{\mu}}{dt} = -\Gamma_{\Delta} \frac{\delta H[\theta_{\mathbf{r}}, \Delta]}{\delta \Delta_{\mu}} + \zeta_{\mu}^{\Delta}, \quad (15)$$

which is identical to the form derived for RSJD [see Eq. (10), where $\Gamma_\Delta = 1/L^d$ was determined from the requirement that no current flows through the boundary]. We here define the dynamic equations for Δ_μ in the RD case with the same value of Γ_Δ , which makes the equations identical to the corresponding equations in RSJD. Within the same interpretation that $I_{\mathbf{r}\mathbf{r}+\hat{\mu}}^n = \dot{\phi}_{\mathbf{r}\mathbf{r}+\hat{\mu}}$ and $I_{\mathbf{r}\mathbf{r}+\hat{\mu}}^s = \sin(\phi_{\mathbf{r}\mathbf{r}+\hat{\mu}})$ with $\phi_{\mathbf{r}\mathbf{r}+\hat{\mu}} = \theta_{\mathbf{r}} - \theta_{\mathbf{r}'} - \Delta_\mu$ as for RSJD (see Sec. II C 1), we are again imposing a condition consistent with that there be no current across the boundary.

In the simulations, the coupled equations of motion are discretized in time (we use the discrete time step $\Delta t = 0.05$ and 0.01 for RSJD and RD, respectively) and numerically integrated using the second order Runge-Kutta-Helfand-Greenside (RKHG) algorithm,¹² which is much more efficient than the first-order Euler algorithm since it can reduce the effective temperature shift⁸ due to the discrete time step significantly. In the case of RSJD we apply the efficient fast Fourier transformation method (see, for example, Ref. 5), which makes the overall computing time $O(L^d \log_2 L)$ in d dimensions. [For comparison, the RD simulation requires $O(L^d)$.] The thermal noises are generated from a uniform distribution, whose width is determined to satisfy the noise correlation (see above) at a given temperature.

III. SCALING RELATIONS

A. Scaling in equilibrium

In order to obtain the dynamic critical exponent z from equilibrium fluctuations of the system we use two different scaling relations: One is the finite-size scaling of the time correlations of the supercurrent and the other is the finite-size scaling of the linear resistance. Fisher *et al.*,¹³ proposed a general scaling theory of the conductivity for a homogeneous superconductor, which has been studied further explicitly by Dorsey and co-worker.^{14,15} The predictions from this scaling theory are very general and depend only on the dynamic scaling assumption and the existence of a diverging correlation length $\xi \sim |T - T_c|^{-\nu}$: From a simple dimensional analysis, it is easy to show that the order parameter scales as $\psi \sim \xi^{1-d/2}$, and thus the superfluid density scales as $\rho_s \sim |\psi|^2 \sim \xi^{2-d}$. Below T_c one has $\sigma(\omega) \sim i\rho_s/\omega$, and accordingly one deduces that the frequency-dependent linear conductivity scales as¹³

$$\sigma(\omega) = \xi^{2-d+z} F_\sigma(\omega \xi^z), \quad (16)$$

where F_σ is a universal scaling function, the dynamic critical exponent z is introduced from $\tau \sim \xi^z$, and τ is the characteristic time scale. Precisely at T_c , Eq. (16) turns into the finite-size scaling form of the conductivity:

$$\sigma(\omega) = L^{2-d+z} F_\sigma(\omega L^z). \quad (17)$$

This scaling relation can be put to practical use in the case of the PBC because for this boundary condition ρ_s has the required size scaling. On the other hand, it cannot be used for an open boundary condition or for the FTBC because in these cases $\rho_s = 0$ at any L and T .⁷ For the FTBC we will then instead use the finite-size scaling of the linear resistance described below.

1. Scaling of supercurrent correlations

The conductivity $\sigma(\omega)$ may be related to the supercurrent correlation function $G(t)$, which for the XY model in d dimensions is given by

$$G(t) = \frac{1}{L^d} \langle F(t)F(0) \rangle, \quad (18)$$

where the global supercurrent $F(t)$ flowing in a given direction, say, \hat{x} , is written as

$$F(t) = \sum_{\mathbf{r}} \sin(\theta_{\mathbf{r}} - \theta_{\mathbf{r}+\hat{x}}). \quad (19)$$

The correlation function $G(t)$ is a key quantity in describing the dynamic response of vortex fluctuations and is for $t = 0$ directly related to the static helicity modulus.⁷ The connection between $\sigma(\omega)$ and $G(t)$ in the RSJD case is expressed as⁸

$$\sigma(\omega) = 1 + \frac{i\rho_s}{\omega} - \frac{1}{T} \int_0^\infty dt e^{i\omega t} G(t), \quad (20)$$

where the conductivity is measured in units such that the shunt resistance $R_0 = 1$, and the superfluid density ρ_s is given by

$$\rho_s = \rho_0 \left(1 - \frac{1}{\rho_0 T} G(t=0) \right), \quad (21)$$

with the bare superfluid density $\rho_0 \equiv \langle \cos(\theta_{\mathbf{r}} - \theta_{\mathbf{r}+\hat{x}}) \rangle$. The dynamic dielectric function $1/\epsilon(\omega)$ in 2D is also expressed as¹⁶

$$\text{Re} \left[\frac{1}{\epsilon(\omega)} \right] = \frac{1}{\epsilon(0)} + \frac{\omega}{\rho_0 T} \int_0^\infty dt \sin \omega t G(t), \quad (22)$$

$$\text{Im} \left[\frac{1}{\epsilon(\omega)} \right] = -\frac{\omega}{\rho_0 T} \int_0^\infty dt \cos \omega t G(t), \quad (23)$$

where

$$\frac{1}{\epsilon(0)} = 1 - \frac{1}{\rho_0 T} G(0). \quad (24)$$

The helicity modulus γ corresponds to the superfluid density ρ_s and is given by $\gamma = \rho_s = \rho_0/\epsilon(0)$. The conductivity $\sigma(\omega)$ in RSJD can be further simplified into the form⁸

$$\sigma(\omega) = 1 - \frac{1}{i\omega} \frac{\rho_0}{\epsilon(\omega)}. \quad (25)$$

Expressing the scaling in terms of $G(t)$ leads to the scaling form

$$G(t) = \xi^{2-d} F_G(t\xi^{-z}), \quad (26)$$

which at T_c for 3D turns into the finite-size scaling form (see Appendix A)

$$LG(t) = F_G(tL^{-z}), \quad (27)$$

while in 2D a logarithmic correction (see Appendix A) needs to be included

$$\ln\left(\frac{L}{c}\right) G(t) = F_G(tL^{-z}), \quad (28)$$

where $F_G(x)$ is the scaling function for $G(t)$. In the following we will use the scaling relations Eqs. (26) and (27) in 3D with the PBC and Eq. (28) in 2D with the PBC.

2. Resistance scaling

In order to obtain a finite-size scaling at criticality for the FTBC for which, like for any open boundary condition, $\rho_s = 0$ at any temperature and any lattice size, we relate the resistance R to the fluctuations of the twist over the sample. The voltage across the sample in the $\hat{\mu}$

direction $V_\mu = -L\dot{\Delta}_\mu$ (see Ref. 8) and the linear resistance R_μ in the same direction are related to the voltage fluctuation by the fluctuation-dissipation theorem¹⁷

$$R_\mu = \frac{1}{2T} \int_{-\infty}^{\infty} dt \langle V_\mu(t) V_\mu(0) \rangle \quad (29)$$

$$\approx \frac{L^2}{2T} \frac{1}{\Theta} \langle [\Delta_\mu(\Theta) - \Delta_\mu(0)]^2 \rangle, \quad (30)$$

where the approximation becomes exact for a sufficiently large time Θ , as shown in Appendix B (a similar approximation has been used for RSJD with open boundary condition in Ref. 18). In the present simulation we use $\Theta = 2000$ and perform average over all d directions, i.e., $R = (\sum_\mu R_\mu)/d$.

Since R_μ scales as the inverse of the characteristic time scale in the critical region, the finite-size scaling takes the form³⁹

$$R = \frac{1}{L^z} F_R((T - T_c)L^{1/\nu}), \quad (31)$$

where ν is the critical exponent for correlation length ($\xi \sim |T - T_c|^{-\nu}$) and $F_R(x)$ is the scaling function for R . Precisely at T_c , $F_R(x) = F_R(0)$ becomes a constant independent of L and we get

$$R \sim L^{-z}, \quad (32)$$

which can be used to determine z , once T_c is known. The resistance scaling can also be turned into an *intersection method*³⁹ for determining z and T_c using that

$$\frac{\ln(R_L/R_{L'})}{\ln(L/L')} = -z + \frac{\ln\left[F_R((T - T_c)L^{1/\nu})/F_R((T - T_c)L'^{1/\nu})\right]}{\ln(L/L')}, \quad (33)$$

for two different lattice sizes L, L' . Thus, if we plot $\ln(R_L/R_{L'})/\ln(L/L')$ as a function of temperature for several pairs of sizes (L, L') , all curves intersect at a single unique point $(T_c, -z)$.³⁹ Once T_c and z are determined through the above intersection method, all data can be made to collapse onto a single scaling curve by plotting RL^z as a function of the scaling variable $(T - T_c)L^{1/\nu}$ with the correct value of the exponent ν [see Eq. (31)].

B. Scaling of relaxation towards equilibrium: Short-time relaxation

Recently, it has been found that a universal scaling in time can also be constructed for the relaxation towards equilibrium when starting from a nonequilibrium configuration. Since such a relaxation is usually rather fast, it is often referred as the short-time relaxation method.²⁰

By this method several critical exponents have been successfully determined for the unfrustrated and the fully frustrated Josephson junction array²¹ as well as for the Ising model.^{20,22} In these studies Glauber dynamics in MC simulations has been used to obtain time series of measured quantities, such as the magnetization and the Binder's cumulant. Here we apply this method to the XY models with more realistic dynamics, RSJD and RD, both introduced in Sec. II C, in order to determine the value of the dynamic critical exponent z . For convenience we measure²²

$$\tilde{\psi} = \left\langle \text{sign} \left[\sum_{\mathbf{r}} \cos \theta_{\mathbf{r}}(t) \right] \right\rangle, \quad (34)$$

starting from the initial condition $\theta_{\mathbf{r}}(0) = 0$. Since $\tilde{\psi}(t=0) = 1$ at any system size L , the finite-size scaling form becomes

$$\tilde{\psi}(t, T, L) = F_\psi(t/L^z, (T - T_c)L^{1/\nu}), \quad (35)$$

with the scaling function $F_\psi(x, y)$ depending on two scaling variables, satisfying $F_\psi(0, y) = 1$ at any y . At T_c , z is easily determined from Eq. (35) because in this case the second argument of the scaling function vanishes and $\tilde{\psi}(t)$ curves obtained for different sizes can be collapsed onto a single curve when plotted against the variable t/L^z . We can also determine T_c by an intersection method similar to Eq. (33) as follows: If the first argument of the scaling function is fixed to a constant ($t/L^z = a$) for a given system size L and z , then $\tilde{\psi}$ has only one scaling variable $(T - T_c)L^{1/\nu}$, and can thus be written as

$$\tilde{\psi} = F_\psi(a, (T - T_c)L^{1/\nu}). \quad (36)$$

Accordingly, if we plot $\tilde{\psi}$ with fixed a as a function of T for various L , all curves should intersect at T_c . However, because a depends on the value of z which cannot be independently determined by this method we start the intersection method from the z value determined from the scaling collapse at T_c . The values of T_c and z obtained from this intersection method can be refined by the iterating intersection construction. Finally, to examine the consistency we collapse the data for all temperatures and lattice sizes onto a single scaling curve in the variable $(T - T_c)L^{1/\nu}$ at fixed $a = t/L^z$, which in addition is a check of the consistency against the known value of the static exponent ν .

IV. SIMULATION RESULTS

A. 2D XY model

In two dimensions, there has been some controversy over the value of the dynamic critical exponent: There has been a theoretical approach by Ambegaokar, Halperin, Nelson, and Siggia²³ (AHNS) predicting $z_{\text{AHNS}} = 1/2\tilde{\epsilon}T^{\text{CG}}$, where the Coulomb gas (CG) temperature $T^{\text{CG}} \equiv T/2\pi\rho_0$ and $1/\tilde{\epsilon} \equiv 1/\epsilon(0)$ (see Sec. III A 1). On the other hand, a simple scaling argument has yielded $z_{\text{scale}} = 1/\tilde{\epsilon}T^{\text{CG}} - 2$.²⁴ Also, in numerical simulations, there have been some differences: On the one hand, z_{AHNS} has been observed in Ref. 25 from RSJ simulations, while z_{scale} has been concluded for RSJD and RD (Refs. 8 and 24), for Langevin dynamics of CG gas particles (Ref. 26), and for the MC simulation of lattice CG (Ref. 19). Although the question is not completely resolved yet, we strongly believe that when the fluctuating twist boundary condition⁸ (see Ref. 27 for a comparison between a conventional boundary condition and the FTBC) is used, z_{scale} is the correct result. Although the above mentioned two z values are different below the KT transition, they give the same value of 2 at the KT transition. In Ref. 28, however, $z \approx 1$ was concluded from a simulation of RSJ dynamics with the

PBC, while in Refs. 29 and 30 a very large value $z \approx 5$ has been suggested from a scaling analysis of existing experimental data and from an analytic calculation using Mori's technique, respectively.

In the low-temperature phase of the 2D XY model, we can alternatively derive z_{scale} in the following way: The potential barrier, which a bound vortex-antivortex pair should overcome in order to escape, is given by

$$\Delta V = \frac{T}{\tilde{\epsilon}T^{\text{CG}}} \ln L,$$

and the escape ratio $\Gamma \sim \exp(-\Delta V/T)$ for one pair is simply related to the total probability of escape, P , by

$$P = L^2 n \Gamma,$$

where n is the vortex pair density. The time scale τ of the system is inversely proportional to P and thus is given by

$$\tau \sim \frac{\exp(\Delta V/T)}{L^2 n} \sim L^{1/\tilde{\epsilon}T^{\text{CG}} - 2} \sim L^z$$

and we obtain the dynamic critical exponent

$$z = \frac{1}{\tilde{\epsilon}T^{\text{CG}}} - 2$$

in accordance with Ref. 24, where z has been obtained from a simple scaling argument and the observed $1/t$ behavior of the correlation function $G(t)$.

In this section, we investigate the dynamic critical exponent of the 2D XY model with RSJD and RD at, below, and above the KT transition. We use the FTBC as well as the conventional PBC and use various methods such as the resistance scaling, the scaling of the supercurrent correlation function, and the short-time relaxation method. The results are summarized in Table I. As seen from Table I only the FTBC gives results in accordance with the expected value: $z_{\text{scale}} = z_{\text{AHNS}} \approx 2$ at $T = 0.90 (\approx T_c)$,³¹ whereas $z_{\text{scale}} \approx 3.4$ and $z_{\text{AHNS}} \approx 2.8$ at $T = 0.80$.⁸ Furthermore, this is the case both for RD and RSJD. In contrast, the results for the PBC are inconsistent both with z_{scale} and z_{AHNS} . From this we conclude that the FTBC is an adequate boundary condition in the context of open systems like superfluid and superconducting films. It is also interesting to note that also the short-time relaxation method for RSJD with the FTBC gives results consistent with z_{scale} . The results in Table I will be further discussed in Sec. V. In the following we present the simulation results on which Table I is based.

1. Critical temperature

First we fix the temperature to $T = 0.90 \approx T_c$ and focus on the dynamic critical behaviors at the KT transition. The results from the resistance scaling $R \propto L^{-z}$

for the FTBC (see Sec. III A 2) are displayed in Fig. 1 (the data points are taken from Ref. 8), where the slopes of the lines in the log-log plot correspond to $z \approx 2$ for both RSJD and RD. Consequently, our result $z \approx 2.0$ is in accordance with other existing theoretical predictions^{23,24} while it contradicts recently suggested, very large values in Refs. 29 and 30.

In order to determine z at the KT transition for the PBC we use the following finite-size scaling form Eq. (28) (see Sec. III A 1) of the supercurrent correlation function $G(t)$

$$\ln\left(\frac{L}{c}\right)G(t) = F_G(tL^{-z}).$$

Figure 2 shows the corresponding scaling plot at $T = 0.90 \approx T_c$ both for RSJD and RD [Figs. 2(a) and (b), respectively]. Very good scaling collapses are obtained in both cases with $z = 1.5$ for RSJD and $z = 2.0$ for RD. This clearly demonstrates that the value of z for RSJD with the PBC is different from the expected value of 2 which was obtained with the FTBC. In these scaling collapses one should note that the relaxation is much faster for RD than for RSJD, as is apparent by comparing the scales on the horizontal axes [note that vertical axis is in a logarithmic scale in Fig. 2(a) and in a linear scale in Fig. 2(b)]. It is also interesting to note that the value of the constant c in the logarithmic correction of Eq. (28) comes from the static properties, as described in Appendix A, and consequently should be independent of the dynamics. In accordance with this expectation the good scalings in Fig. 2 are achieved with the same value of c : Both for RSJD in Fig. 2(a) and for RD in Fig. 2(b), we found that $c = 0.60$ gives a good collapse.

In Fig. 3, we next show the decay of $\tilde{\psi}$ (see Sec. III B for details) at $T = 0.90 \approx T_c$ for RSJD with the (a) FTBC and (b) PBC, which demonstrates that $z \approx 2.0$ (for the FTBC) and $z \approx 1.2$ (for the PBC) result in good data collapses to scaling curves. However, only the FTBC leads to the expected value $z \approx 2.0$. One should also note that the PBC results in an extremely slow decay of $\tilde{\psi}$. Similarly Fig. 4 shows the decay of $\tilde{\psi}$ for RD at $T = 0.90$ with the (a) FTBC and (b) PBC. In both cases good data collapses are obtained for $z \approx 2.0$. In this case of RD, both boundary conditions have the same magnitude of the decay time scale. A possible interpretation is discussed in Sec. V.

2. Low-temperature phase

The 2D XY model is special in that the whole low-temperature phase is “quasi” critical. This means that each temperature in the low-temperature phase is characterized by a temperature-dependent dynamic critical exponent z . Just as in the previous section, this temperature-dependent z can be determined from the size scaling of the linear resistance, i.e., $R \propto L^{-z}$.

Figure 5 shows the finite-size scaling of resistance at $T = 0.8 (< T_c)$ for 2D RSJD and RD with the FTBC (all data are from Ref. 8) and we find $z \approx 3.3$ for both types of dynamics. In Ref. 8, this value has been compared with z_{scale} and z_{AHNS} at this temperature and it has been concluded that the observed value 3.3 is very close to $z_{\text{scale}} \approx 3.4$.

In the same way as in the previous section the temperature-dependent z in the low-temperature phase can also be probed by the short-time relaxation method described in Sec. III B. The divergence of the correlation length in the whole low-temperature phase in 2D turns the finite-size scaling form (35) into the simpler form

$$\tilde{\psi} = F_\psi(t/L^z), \quad (37)$$

with the temperature-dependent z . Figures 6 and 7 show the finite-size scaling of the short-time relaxation at $T = 0.80$ with the (a) FTBC and (b) PBC. The value $z \approx 3.2$ found in Fig. 6(a) for RSJD with the FTBC is in agreement with $z \approx 3.3$ obtained from the resistance scaling in Fig. 5 within numerical accuracy. We interpret this as an evidence that z for the RSJD with the FTBC is indeed given by z_{scale} . This is in contrast to the RSJD with the PBC for which at the same temperature ($T = 0.80$) $z \approx 1.4$ is determined from short-time relaxation as shown in Fig. 6(b). As will be discussed in Sec. V, we interpret this as further evidence that, in case of the 2D RSJD, z does depend on the boundary condition. The short-time relaxation for RD gives a quite different result: $z \approx 2$ is obtained for $T = 0.80$ for both the FTBC and PBC, as shown in Fig. 7. If one compares this with the results at T_c in Fig. 4, where $z \approx 2$ is also obtained, the implication is that the result $z \approx 2$ for the short-time relaxation is expected at any temperature in the low-temperature phase both for the FTBC and PBC. As will be discussed further in Sec. V, this suggests that the short-time relaxation for RD does not probe the true equilibrium critical dynamics.

3. High-temperature phase

In the high-temperature phase there is a finite screening length ξ which diverges as T_c is approached from above. Close to T_c one then expects that the characteristic time scales as

$$\tau \sim \xi^z.$$

In case of the PBC, we can estimate ξ and τ following the method in Ref. 32: ξ is obtained from the wavevector dependence of the static dielectric function $1/\epsilon(0)$ introduced in Eq. (24). The characteristic frequency $\omega_0 \sim 1/\tau$ is determined from the frequency dependence of $1/\epsilon(\omega)$; ω_0 is the position of the dissipation peak in $|\text{Im}1/\epsilon(\omega)|$. The result for RSJD with the PBC is shown in Fig. 8, where $z \approx 2$ is found from $\omega_0 \sim \xi^{-z}$. It should be noted

that since this result is obtained for a temperature range where $\xi/L \ll 1$ it is expected to be independent of the treatment of the boundary and hence applies to both the PBC and FTBC. The same method applied to RD also gives $z \approx 2.0$ as shown in Ref. 32. In Fig. 8 the dotted line with slope -1 is also shown and corresponds to the result in Ref. 28, where $z \approx 1$ was obtained for RSJD with the PBC in the same temperature range. Consequently, Fig. 8 implies, in contrast to Ref. 28, that $z = 2$ is the correct value for the PBC as well as for the FTBC, when z is determined from $\tau \sim \xi^z$.

B. 3D XY model

Next we turn to the 3D XY model with current conserving RSJD and nonconserving RD, respectively. Both dynamic models have been used to describe the dynamic properties of high T_c superconductors. Whereas it is generally agreed upon that the static critical properties are those of the 3D XY model in a region close to T_c with the corresponding static critical exponents,³³ there is less consensus on the dynamic critical properties. Several seemingly mutually inconsistent experimental^{34–37} and simulational^{19,38,39} results have been reported. Similarly to the 2D case described above in Sec. IV A, we will here arrive at a somewhat entangled picture by comparing values of z obtained from the scalings in equilibrium for the two types of dynamics (RSJD and RD) with the two types of boundary conditions (the PBC and FTBC), as well as from the short-time relaxation method by observing the time evolution towards equilibrium when starting from a nonequilibrium configuration. For convenience, the results of the simulations for the 3D XY model are summarized in Table II.

1. Resistance scaling

We start with the determination of z for the FTBC using the finite-size scaling of the linear resistance, which is calculated from the equilibrium fluctuation of twist variable Δ [see Eq. (30)]. A shorter presentation of these results has also been given in Ref. 40. In 3D the correlation length diverges as $\xi \sim |T - T_c|^{-\nu}$, making the extended scaling form of Eq. (31), as well as the intersection method in Eq. (33) applicable in addition to the relation $R \sim L^{-z}$ at T_c .

We first present the result for the scaling of the linear resistance for RSJD with the FTBC. By using the intersection method explained in Sec. III A 2 [see Eq. (33)] we determine T_c and z simultaneously from the unique intersection point, as shown in the inset of Fig. 9, which yields $T_c \approx 2.200$ and $z \approx 1.46$. We then display in the main part of Fig. 9 the scaling plot of the linear resistance [see Eq. (31)], RL^z as a function of the scaling variable $(T - T_c)L^{1/\nu}$, at $T = 2.17, 2.19, 2.20, 2.21,$ and 2.23 for

$L = 4, 8,$ and 16 . Here we used z and T_c found from the intersection method, i.e., $z = 1.46$ and $T_c = 2.200$, respectively, and the known value of the static exponent $\nu \approx 0.67$.³¹ We also tried to vary the values of $T_c, z,$ and ν in the scaling plot and concluded that $z = 1.46 \pm 0.06$ for the case of 3D RSJD with the FTBC. It is noteworthy that $T_c \approx 2.200$ from the intersection method is very close to the known value of $T_c [\approx 2.2018$ (Ref. 31)] from the MC simulation.

For RD with the FTBC we only focus on the scaling relation $R \sim L^{-z}$ at T_c , since it is found that the resistance for the RD case is harder to converge due to a sensitivity of the result on the discrete time step in the numerical integration of dynamic equations even when using the second-order RKHG algorithm.¹² In contrast, we did not observe any significant sensitivity to the time step in RSJD and we fix $\Delta t = 0.05$ throughout the present work for RSJD. In order to overcome the problem in RD due to the finite-time step we obtain data for two different time steps ($\Delta t = 0.05, 0.01$) and linearly extrapolate to $\Delta t = 0$, as shown in Fig. 9(b) for $L = 4, 6, 8, 10, 12,$ and 16 . The slope of the line in the log-log plot of R versus L in Fig. 9(b) gives $z \approx 1.5$ also for 3D RD with the FTBC.

2. Supercurrent scaling

For the PBC we use the scaling of the supercurrent correlation function $G(t)$ introduced in Sec. III A 1 in order to obtain z . In Fig. 10(a) we use the finite-size scaling form in Eq. (27) and plot LG as a function of the scaling variable t/L^z for (a) $L = 8, 16,$ and 24 for RSJD and (b) $L = 6, 8, 12, 16,$ and 24 for RD, respectively: Optimal data collapse is achieved for $z = 1.5$ (RSJD), and $z = 2.05$ (RD), respectively. In the insets of Fig. 10 we use (a) $z = 2.0$ for RSJD and (b) $z = 1.5$ for RD, respectively, and show that the data collapse becomes significantly worse and consequently conclude that the z values obtained by this data collapse method are well determined [see the main parts of Figs. 10(a) and 10(b)]. One notes that for RSJD $z \approx 1.5$ is obtained for both the FTBC and PBC, whereas for RD $z \approx 1.5$ and $z \approx 2$ are obtained for the FTBC and PBC, respectively.

In the critical region above T_c where $\xi \ll L$ we instead have $\xi G(t)$ as a scaling function with the scaling variable t/ξ^z [see Eq. (26)]. Figure 11 shows this scaling results at temperatures above T_c ($T = 2.25, 2.30,$ and 2.40) for $L = 24$. By comparing with the results for $L = 32$, it is explicitly checked that there remain no significant finite-size effects in the current temperature range. In Fig. 11 the corresponding values of ξ are taken from high precision MC simulations.⁴¹ As shown in Fig. 11, the optimal value $z = 1.4(2)$ is found for RSJD and $z = 1.9(2)$ for RD, respectively, which is consistent with the finite-size scaling of $G(t)$ at T_c . However, we note that the determination of z in the case of the finite- ξ scaling above T_c yields a somewhat larger uncertainty.

Furthermore, $z \approx 2$ found for RD with the PBC is particularly intriguing to understand since we expect that this result should be independent of boundary condition in this high-temperature regime where $\xi \ll L$: Thus one expects the same value $z \approx 2$ for the FTBC in this high-temperature regime. This in turn suggests a discontinuous jump in the z value from $z \approx 2$ to $z \approx 1.5$ as T_c is approached from above, since $z \approx 1.5$ at T_c was observed in the scaling of the linear resistance in Sec. IV B 1. This possibility is also discussed in Sec. V.

3. Short-time relaxation scaling

The short-time relaxation method described in Sec. III B probes the relaxation towards equilibrium from a nonequilibrium configuration. We start with the presentation of the results obtained for RSJD and RD with the FTBC. Using the scaling form of $\tilde{\psi}$ in Eq. (35) at T_c , where the scaling function has only one scaling variable t/L^z , we first show in Fig. 12 the scaling plot of $\tilde{\psi}$ at $T = 2.20$ for (a) RSJD with $L = 4, 8,$ and 16 and (b) RD with $L = 6, 8,$ and $10,$ respectively. All the data can be made to collapse onto a single curve in a broad range of the scaling variable for $z \approx 1.5$ and $z \approx 2.0$ for RSJD and RD, respectively. However, the above method presumes *a priori* knowledge of T_c . To circumvent this, one can alternatively use an intersection method with a fixed value of $a = tL^{-z}$ in the first argument of the scaling form in Eq. (36) (see Sec. III B). In insets of Fig. 13 we display data points at $T = 2.17, 2.19, 2.20, 2.21,$ and 2.23 for (a) RSJD with $L = 4, 6, 8,$ and 16 and (b) RD with $L = 4, 6, 8,$ and $10,$ and show the results of the iterative intersection method. We obtain again $z \approx 1.5$ and $z \approx 2.0,$ as well as the estimations of the critical temperatures $T_c \approx 2.200$ and $T_c \approx 2.194$ for (a) RSJD and (b) RD, respectively. We believe that the existence of an unique intersection point in each dynamics with the value $T_c \approx 2.200$ obtained for RSJD, which is in very good agreement with $T_c \approx 2.200$ obtained previously from the resistance scaling, and with $T_c \approx 2.2018$ from MC simulations,³¹ make this short-time relaxation method very reliable. One notes that the slight temperature shift for RD is again the effect of the finite time step, as already observed in the calculation of the linear resistance. We have also checked the dependence on a values and observed no significant changes in resulting values of T_c and z in a broad range where $0.4 < \tilde{\psi} < 0.9$. Using z and T_c found from the intersection method, we in Fig. 13 confirm that the full scaling form is borne out to high precision with $\nu = 0.67$ determined from MC simulations.³¹

We next consider the short-time relaxation for PBC, and show in Fig. 14 the scaling plot at $T = 2.20,$ $\tilde{\psi} = F_\psi(t/L^z),$ for (a) RSJD and (b) RD. Treating z as a free parameter, we obtain $z \approx 1.2$ and $z \approx 2$ for RSJD and RD, respectively. This suggests that the value for

RSJD with the PBC is lower than $z \approx 1.5$ obtained from the same short-time relaxation method for RSJD with the FTBC, whereas for RD a value $z \approx 2$ is obtained both for the FTBC and PBC. As already observed in 2D, RSJD with the PBC has a very large decay time scale in contrast to RSJD with the FTBC as well as to RD with both the PBC and FTBC.

C. 4D XY model

For completeness we also determine z in 4D.⁴² As a prerequisite we first estimate T_c through the use of MC simulations in conjunction with the finite-size scaling analysis of the Binder's fourth-order cumulant⁴³ $U,$ which is independent of L precisely at $T_c,$

$$U(L, T) = 1 - \frac{\langle |m|^4 \rangle}{3 \langle |m|^2 \rangle^2},$$

with the order parameter $m = \sum_{\mathbf{r}} e^{i\theta_{\mathbf{r}}}/L^4.$ The results are shown in Fig. 15 and $T_c \approx 3.31$ is found from MC simulation with the PBC, which is consistent with earlier reports⁴⁴ but has a higher accuracy. From the MC simulations we also verified that ν in 4D has the expected mean-field value $\nu = 1/2$ (see, e.g., Ref. 45). Since, as noted in the previous section, the size of the discrete time step in the integration of the dynamic equations of motion can lead to an effective increase of temperature, we explicitly determine the effective T_c for RSJD and RD with the time step $\Delta t = 0.05$ from the crossing point of $U(L, T):$ Figure 15 shows that there is no significant difference between the effective and nominal temperature for RSJD, leading to $T_c(\text{RSJD}) \approx T_c(\text{MC}) \approx 3.31.$ On the other hand, for RD we from the crossing point obtain $T_c \approx 3.25$ at the same time step $\Delta t = 0.05,$ in parallel with what was found for RD in 3D. It is to be noted that although the above critical temperatures have been obtained only with the PBC, the same critical temperature is expected also for the FTBC since all static quantities such as T_c should not depend on boundary conditions used.

Once T_c is known from the calculation of the Binder's cumulant, we can use the simple finite-size scaling form Eq. (32) for the linear resistance calculated with the FTBC by Eq. (30) (we use $\Theta = 2000$ for both RSJD and RD). In Fig. 16(a), we plot the linear resistance R versus L at $T = 3.31$ (RSJD) and $T = 3.25$ (RD), and from the least-square fit we find $z \approx 2.1$ for RSJD and $z \approx 2$ for RD, respectively. In addition, we also measure the short-time relaxation with the FTBC and present the result for RD at $L = 6$ and 8 in the inset of Fig. 16(a) by using the simple scaling form at $T = T_c = 3.25,$ i.e., $\tilde{\psi} = F_\psi(tL^{-z}),$ which yields $z \approx 2.0$ in accordance with the result from the resistance scaling. For RSJD with the FTBC, we construct the intersection plot for the short-time relaxation (similar to Fig. 13 for 3D) as displayed in the inset of Fig. 16(b), and get $z \approx 2.0$ and $T_c \approx 3.31$ from

the unique crossing point. It is interesting to note that the critical temperature obtained here for RSJD with the FTBC is in a perfect agreement with T_c found from the Binder's cumulant method for the other boundary condition, the PBC. We then make the full scaling plot for $\tilde{\psi}$ in the main part of Fig. 16(b) with the mean-field value $\nu = 0.5$ and the estimated values $T_c = 3.31$ and $z = 2.0$ above, resulting in a very smooth collapse.

In short, we get $z \approx 2$ in 4D with the FTBC regardless of the dynamics we use (see Table III for a summary of results); this is reassuring since the value $z = 2$ is usually expected in 4D where the phase transition acquires a mean-field nature.^{11,45}

V. DISCUSSIONS AND COMPARISONS

As is clear from the simulation results presented in Sec. IV for two-, three-, and four-dimensional XY models, a very entangled picture emerges as regards to the dynamic critical exponent z . In this section we discuss the main features.

A. Discussions of the 2D XY model

We start our discussion with 2D (see Table I for summary of results) and first focus on RSJD at the KT transition. For a 2D superfluid and superconductor the most widely expected value is $z = 2$ although there have been a few different suggestions (Refs. 28–30). The value $z = 2$ can be inferred from the observed nonlinear current-voltage (I - V) exponent $a = 3$ (Refs. 8,24,26, and 46) together with the scaling argument that $a = z + 1$.^{13,14} It may also be directly obtained from the simple argument of the escape over the boundary presented in Sec. IV A with the result $z = 1/\tilde{\epsilon}T^{CG} - 2$, combined with the universal jump condition at the KT transition $1/\tilde{\epsilon}T^{CG} = 4$,^{2,47,48} which leads to $z = 2$ at the transition. For the 2D XY model, the KT transition temperature is $T_c \approx 0.9$ (Ref. 31) and as seen from Table I, RSJD with the FTBC does give the expected value. However, RSJD with the conventional PBC does in fact not give the expected value: the supercurrent scaling gives $z \approx 1.5$ and the short-time relaxation gives $z \approx 1.2$.

In order to understand the role played by the boundary conditions we consider a system with an open boundary, which is appropriate to describe a superconducting film and a film of ^4He in usual experiments. In such a case, when a vortex-antivortex pair is introduced into the ground state and then annihilated across the boundary, the system relaxes back to the original ground state. The FTBC has been designed to keep the advantage of the PBC, which reduces the finite-size effect compared to the free boundary condition, as much as possible, while allowing this relaxing back. This relaxing back is, however, prohibited by the conventional PBC.⁷ One may note that

the escape-over-barrier argument in Sec. IV A implicitly presumes this relaxation back as a part of the escape process. One should also note that, when comparing to experiments with open boundaries, the FTBC has to be used in simulations instead of the PBC whenever the relaxation process across the boundary is important. This perspective suggests that the observed difference between the FTBC and PBC at the KT transition for RSJD is due to the additional constraint on the physics caused by the PBC.

This can be substantiated somewhat further by studying the low-temperature phase in 2D, where an ubiquitous “quasi” criticality with a diverging correlation length makes the critical finite-size scaling method applicable. In Ref. 8, $z \approx 3.3$ at $T = 0.80$ was found for the FTBC from the resistance scaling in agreement with the expected value $z = 1/\tilde{\epsilon}T^{CG} - 2 \approx 3.4$ within numerical errors. However, an estimate of the equilibrium scaling for the PBC at $T = 0.85$ in Ref. 8 gave $z \approx 1.6$ instead of the expected result $z \approx 2.8$ (see Fig. 3 in Ref. 8). Thus in this low-temperature phase z determined with the PBC appears to be smaller ($z < 2$) than the one with the FTBC ($z > 2$). However, the value for the FTBC is the relevant one when comparing with experiments.

The situation above T_c is as follows: The finite linear resistance R calculated from the fluctuations of Δ for the FTBC [see Eq. (30)] can be related to the conductivity calculated for the PBC through the connection $R = \text{Re}[1/\sigma(\omega = 0)]$ with $\sigma(\omega)$ in Eq. (20). We have explicitly checked this relation in our simulations at $T = 1.4$, by comparing the two values for the FTBC and PBC, respectively, and found good agreement.⁴⁹ From this observation, we expect that in this high-temperature phase where the correlation length is smaller than the linear size of the system, R and z are independent of boundary conditions. Furthermore, in this temperature regime, transport properties like the linear resistance are dominated by free vortices (with density n_F) and accordingly we expect $R \propto n_F \propto \xi^{-2}$ (Ref. 2), leading to $z = 2$ for both boundary conditions. However, from a computational point of view, the calculation of the size-converged R for the FTBC in the high-temperature phase becomes difficult as we approach T_c from above, due to the diverging correlation length. On the other hand, if we instead focus on the scaling of the characteristic frequency ω_0 , which is expected to be proportional to R and can be calculated for the PBC, then we do indeed find an indication of the expected behavior, $\omega_0 \sim \xi^{-2}$, as seen in Fig. 8 for the PBC. For the FTBC this result is consistent with our observation $z \approx 2.0$ at T_c , whereas for the PBC the scaling at T_c gives $z \approx 1.5$, which differs from the expectation. Why is there then a difference in the PBC between z values at and above T_c ? The point is that the long-time relaxation above T_c is governed by the thermally created free vortices, whose density satisfies $n_F \propto \xi^{-2}$, whereas the behavior precisely at T_c , where $n_F = 0$, is instead dominated by the bound pairs of vortices and antivortices. The conclusion is then that the

constraint imposed by the PBC on the vortex-antivortex escape gives rise to this peculiar discontinuity of z precisely at T_c . This is in contrast to the FTBC case where z appears to be a continuous function of T .

Next we compare the results from the dynamic scaling in equilibrium and the short-time relaxation method which probes the relaxation when the system approaches equilibrium. For RSJD with the FTBC there is no difference: the resistance scaling and the short-time relaxation method yield the same z at and below T_c (see Table I). However, for RSJD with the PBC the equilibrium scaling and the short-time relaxation scaling lead to different results, $z \approx 1.5$ and $z \approx 1.2$, respectively. In fact by comparing Figs. 2(a) and 3(b) one realizes that the approach to equilibrium from the chosen starting nonequilibrium configuration is much slower than the equilibrium relaxation. Apparently the constraint imposed on the relaxation by the PBC in combination with the nonequilibrium starting configuration is causing the difference.

We now turn to the discussions for RD, where for the FTBC we find from the resistance scaling the same z at and below T_c as for RSJD (see Table I). In this context it is interesting to note that the 2D XY model with the FTBC is dual to the lattice CG model with the PBC (see Ref. 7 for the mapping between two models), where the same values of the dynamic critical exponent ($z = z_{\text{scale}} = 1/\tilde{\epsilon}T^{\text{CG}} - 2$) have been found in MC dynamics.⁴⁶ Also, the continuum CG model with Langevin dynamics of the pure relaxational form has been found to give the same values of z .²⁶ Accordingly it is tempting to conclude that the result presented in this work for the 2D XY model with the FTBC is associated with the vortices and that it is essential to define the model so as to allow for a proper relaxation of vortex-antivortex annihilation across the boundary, which is not the case for the PBC. Furthermore, the result that $z = z_{\text{scale}}$ appears to be universal in the sense that it does not matter whether or not the underlying dynamics is purely relaxational (such as RD in this work, MC dynamics in Ref. 46, and Langevin dynamics in Ref. 26), or it has an additional constraint like local current conservation in the RSJD case.

Although the short-time relaxation method applied to RD gives the expected value $z \approx 2$ at T_c , it fails to yield the equilibrium size scaling value below T_c . In addition, if we compare the decay behaviors at and below T_c , shown in Figs. 4 and 7, respectively, we notice that the time scale of the relaxation does not depend significantly on the temperature or on the boundary condition, in sharp contrast to RSJD. We suggest the following reason: In RD the relaxations of spin waves and vortices are effectively decoupled and the short-time relaxation in this case only probes the spin-wave degrees of freedom, which follow the purely relaxational dynamics with the trivial exponent $z = 2$ at any T , while the resistance scaling probes the vortex degrees of freedom. This is then in contrast to RSJD with the FTBC where both degrees of freedom are strongly coupled, leading to the same relaxation time (and accordingly the same z value) for $\tilde{\psi}$

and R . It is also interesting to note that $z \approx 2$ was also found in Ref. 21 from the MC simulations of the 2D XY model with the PBC at and below T_c by using a similar short-time relaxation method.

B. Discussions of the 3D XY model

We next turn to the 3D XY model (see Table II for a summary of results). The discussion for the 2D case in Sec. V A regarding the boundary conditions carries over to 3D, and we expect that the FTBC has to be used whenever the relaxation process associated with the expansion and the subsequent annihilation of a vortex loop across the boundary is important because the conventional PBC prevents this relaxation.

For RSJD, $z \approx 1.5$ is found from the linear resistance and the short-time relaxation method for the FTBC, as well as from the scaling of the supercurrent correlation at and above T_c for the PBC. In addition, the same value $z \approx 1.5$ is also found for RD with the FTBC from the finite-size scaling of the linear resistance. We note here that the MC simulations of the lattice vortex loop model in 3D (Ref. 19) also have found the same value. The agreement between the z values for the three different dynamic models (RSJD and RD with the FTBC, and MC dynamics of the vortex loop model with the PBC) was also found in 2D. This value $z \approx 1.5$ obtained in 3D is consistent with $z = d/2$ (with $d = 3$ in 3D) for model E and model F describing critical dynamics of superfluid systems, in the classification scheme of Hohenberg and Halperin.^{11,50} Consequently, it is again tempting to conclude that the result for the 3D XY model can be associated with the vortex loops and that the critical dynamics of RSJD and RD are equivalent as long as the boundary condition allows for the proper vortex loop escape over the boundary.

As in 2D, we find that the short-time relaxation method for RSJD with the PBC (with the result $z \approx 1.2$) does not reflect the true equilibrium relaxation corresponding to $z \approx 1.5$, and we again suggest that this is due to the constraint imposed by the PBC. On the other hand, we find that the short-time relaxation method for RD with the FTBC gives $z = 2.0(1)$ [see Figs. 12(b) and 13(b)]. We propose the same explanation as we did for 2D: The short-time relaxation in RD at criticality does not reflect the true long time relaxation because the vortex loop configurations are still out of equilibrium even when $\tilde{\psi} \approx 0$ is reached. In this respect it is interesting to note that the values $T_c = 2.20$ and $\nu = 0.67$ used in the scaling collapse for $\tilde{\psi}$ in Fig. 13(b) with $z = 2.0$ agree with the value expected for the 3D XY model and that the same $T_c = 2.20$ was used in the resistance scaling in Fig. 9(b) and yielded $z \approx 1.5$.

We next discuss the results for RD with the PBC. The scalings of the supercurrent correlation both at and above T_c (corresponding to the finite- L scaling and the finite- ξ

scaling, respectively), as well as the short-time relaxation at T_c , consistently give $z \approx 2$. This value corresponds to model A of relaxational dynamics in the Hohenberg-Halperin classification scheme.^{11,14,15} The most striking feature in RD is that the scalings at T_c for the FTBC (resistance scaling) and PBC (supercurrent scaling) correspond to different values, i.e., $z \approx 1.5$ and $z \approx 2.0$, respectively.

In the high-temperature phase in 3D where $\xi \ll L$, one expects that z is independent of boundary conditions.⁵¹ Consequently, $z \approx 2$ found for RD with the PBC at temperatures above T_c implies $z \approx 2$ also for RD with the FTBC in the same high-temperature regime, again consistent with model A.¹¹ In contrast, z determined from the resistance scaling at T_c instead gives $z \approx 1.5$ for RD with the FTBC. We propose the same explanation for this discontinuity of z at T_c in the RD case with the FTBC as we did in 2D: Above T_c where $\xi \ll L$, the finite value of the resistivity reflects the physics of dissociated vortex loops whereas precisely at T_c , where the resistivity vanishes as L is increased, the physics is dominated by the large nondissociated vortex loops.

We now compare our results in 3D with earlier studies. Values consistent with $z \approx 1.5$ have also been found in earlier simulations: $z = 1.5(5)$ was obtained from the I - V characteristics of the current-driven RSJ model with an open boundary (Ref. 52), and $z = 1.5(1)$ was concluded from the scaling of the linear resistance for the MC simulations of the XY model in the vortex representation with the PBC (Refs. 19 and 39) which corresponds to the FTBC in the phase representation as mentioned above and explained in Ref. 7. Finally, MC spin dynamics applied to the three component XY model gave $z = 1.38(5)$ in Ref. 53. On the other hand, the experimental situation for high- T_c superconductors is less clear:⁵⁴ From several zero field dc conductivity experiments $z \approx 1.5$ has been found on single YBCO-123 crystals³⁴ and a similar result $z = 1.6(1)$ was also obtained for a Bi-2212 crystal.³⁷ However, from the scaling of the magnetoconductivity of a thick YBCO-123 film $z = 1.25(5)$ was found in Ref. 36, whereas a similar experiment reported $z \approx 2$ in Ref. 55. From a theoretical point of view the renormalization group methods applied to the relaxational model (model A) yield the result $z = 2 + c\eta$,^{11,15} with $\eta \approx 0.02$ and $c \approx 0.7261$, leading to $z \approx 2.0$. However, as far as we know, no corresponding calculation has been made for the 3D RSJ model. One may argue that since the 3D RSJ model is a *bona fide* model of a superconductor the critical dynamics should belong to the dynamic universality class of model F which describes superfluids.¹¹ This gives $z = d/2 = 1.5$ for a model with the static properties given by the 3D XY model.¹¹

C. Discussions of the 4D XY model

In case of the 4D XY model both resistance scaling at T_c and short-time relaxation give $z \approx 2$ for RSJD as well as for RD (see Table III for summary of results). This is in perfect accordance with the Hohenberg-Halperin classification scheme where the RSJD case should be related to models E and F with $z = d/2 = 2$ and the RD case with the model A value $z = 2$. This in turn just reflects that 4D is the upper critical dimension.

VI. SUMMARY

We have found that the size scaling of the resistance for the XY model with the FTBC gives the dynamic critical exponent z related to superfluid and superconducting systems with an open boundary. This is the case in two, three and four dimensions both for relaxational and RSJ dynamics. In 2D this applies for $T \leq T_c$, whereas in 3D and 4D the dynamics is critical only at $T = T_c$. However, the 3D case with relaxational dynamics has a discontinuity in the z value since the relaxation time τ scales as $\tau \propto L^{1.5}$ at T_c , whereas it scales as $\tau \propto \xi^2$ just above T_c .

The short-time relaxation method, which probes the relaxation from a nonequilibrium configuration, does give the same result, except for the 3D case with relaxational dynamics where $z \approx 2$ is obtained. This discrepancy shows that although the short-time relaxation method very often is reliable and efficient, it cannot always be trusted as a determination of the critical equilibrium dynamics.⁵⁶

The XY model with the PBC has a different dynamical size scaling behavior than with the FTBC. In 2D the XY model with the PBC and RSJ dynamics gives smaller values of z ($z < 2$) both at and below T_c . This demonstrates that the boundary condition influences the size scaling properties of the dynamics. Also in this case there is a discontinuity in z since $\tau \propto L^{1.5}$ at T_c but $\tau \propto \xi^2$ just above. This is similar to the discontinuity found in 3D for relaxational dynamics. The short-time relaxation fails to give the equilibrium z at T_c for the 2D XY model with the PBC and RSJ dynamics.

In 3D the XY model with RSJ dynamics and the PBC gives the same result as for the FTBC. Thus in this case the boundary condition does not influence the size scaling. This is in contrast to the 3D XY model with relaxational dynamics which gives different result for the PBC and FTBC.

In 4D all determinations give the simple relaxational value $z \approx 2$ independent of boundary condition and dynamics.

The actual values determined are consistent with the following sequences: the XY model with RSJ dynamics and the PBC at T_c is consistent with $z = 1.5, 1.5,$ and 2 for the 2D, 3D and 4D cases, whereas the FTBC is consistent with $z = 2, 1.5,$ and 2 . Similarly for relaxational

dynamics the PBC gives the sequence $z = 2, 2,$ and 2 whereas the FTBC gives $z = 2, 1.5,$ and $z = 2$ for the 2D, 3D, and 4D cases, respectively.

The z values for a superconductor can be related to the nonlinear I - V exponent a through the scaling relation $a = 1 + z$.^{13,14} The I - V measurements correspond to an open boundary and simulations with the FTBC are consistent with the scaling relation, as shown for the 2D case in Ref. 8. On the other hand, the z values calculated with the PBC in 2D do not fulfill the relation because $a > 1 + z$ for $T \leq T_c$. In this sense, the bound-

ary condition has direct physical significance.

ACKNOWLEDGMENTS

The authors thank P. Olsson for useful discussions and for providing his unpublished high-precision results of Monte Carlo simulations. This work was supported by the Swedish Natural Research Council through Contract No. FU 04040-332.

APPENDIX A: SCALING FORM OF THE SUPERCURRENT CORRELATION FUNCTION

For supercurrent correlation scaling in 2D, the superfluid density ρ_s is proportional to the vortex dielectric function $1/\epsilon(0)$ which in turn is related to the conductivity by $\sigma(\omega) \propto 1/[i\omega\epsilon(\omega)]$. Precisely at the KT transition $1/\epsilon(0)$ has a logarithmic size scaling,⁵⁷

$$\frac{1}{\epsilon_L(0)} - \frac{1}{\epsilon_\infty(0)} \propto \frac{1}{\ln(L/c)}$$

, where c is a constant. This is consistent with the functional form in terms of a scaling function with a logarithmic correction for the frequency dependence

$$\frac{1}{\epsilon(\omega)} - \frac{1}{\epsilon(0)} \propto \frac{1}{\ln(L/c)} F_\epsilon(\omega\tau).$$

The supercurrent correlation function $G(t)$ is related to $\sigma(\omega)$ by a Fourier transform so that

$$\text{Im} \left[\frac{1}{\epsilon(\omega)} \right] = \int_0^\infty dt \omega \cos \omega t G(t) = \frac{\tilde{F}_\epsilon(\omega\tau)}{\ln L/c},$$

where $\tilde{F}(x) = \text{Im}[F(x)]$. From this it follows that

$$\ln(L/c)G(t) \propto \int_{-\infty}^\infty d\omega \frac{1}{\omega} \tilde{F}_\epsilon(\omega\tau) e^{-i\omega\tau t/\tau} = \int_{-\infty}^\infty d\omega\tau \frac{1}{\omega\tau} \tilde{F}_\epsilon(\omega\tau) e^{-i\omega\tau t/\tau} = F_G(t/\tau),$$

so that $\ln(L/c)G(t)$ has the scaling form $F_G(t/\tau)$.

In 3D we have instead $1/\epsilon_L(0) \propto \rho_s \propto 1/L$ at T_c and $1/\epsilon_\infty(0) = 0$ so that this time $1/\epsilon_L(0) - 1/\epsilon_\infty(0) \propto 1/L$. This means that going through the same steps as above for the 3D case gives the scaling form $LG(t) = F_G(t/\tau)$.

APPENDIX B: APPROXIMATION MADE IN THE NYQUIST FORMULA FOR LINEAR RESISTANCE

The step from Eq. (29) to Eq. (30) is equivalent to showing that

$$\int_0^\Theta dt \langle \dot{\Delta}(t) \dot{\Delta}(0) \rangle \rightarrow \frac{1}{2\Theta} \langle (\Delta(\Theta) - \Delta(0))^2 \rangle$$

in the limit of large Θ . The left-hand side can, due to translational invariance, be written as

$$\frac{1}{\Theta} \int_0^\Theta ds \int_0^\Theta dt \langle \dot{\Delta}(t+s) \dot{\Delta}(s) \rangle = \frac{1}{\Theta} \int_0^\Theta ds \left[\int_{-s}^{\Theta-s} - \int_{-s}^0 + \int_{\Theta-s}^\Theta \right] dt \langle \dot{\Delta}(t+s) \dot{\Delta}(s) \rangle. \quad (\text{B1})$$

The first term on the right-hand side is $\langle (\Delta(\Theta) - \Delta(0))^2 \rangle / \Theta$, and the second term reduces to

$$-\frac{1}{\Theta} \int_0^\Theta ds \int_{-s}^0 dt \langle \dot{\Delta}(t+s) \dot{\Delta}(s) \rangle = -\frac{1}{\Theta} \int_0^\Theta ds \langle [\Delta(s) - \Delta(0)] \dot{\Delta}(s) \rangle \quad (\text{B2})$$

$$= -\frac{\langle \Delta^2(\Theta) - \Delta^2(0) - 2\Delta(0)\Delta(\Theta) + 2\Delta^2(0) \rangle}{2\Theta} \quad (\text{B3})$$

$$= -\frac{\langle [\Delta(\Theta) - \Delta(0)]^2 \rangle}{2\Theta}, \quad (\text{B4})$$

where we have used $2\Delta(s)\dot{\Delta}(s) = d\Delta^2/ds$. Thus the sum of the first two terms on the right-hand side of Eq. (B1) is equal to $\langle [\Delta(\Theta) - \Delta(0)]^2 \rangle / 2\Theta$ and it remains to prove that the third term vanishes in the limit $\Theta \rightarrow \infty$. This can be realized by changing the order of integration:

$$\frac{1}{\Theta} \int_0^\Theta ds \int_{-s}^0 dt \langle \dot{\Delta}(\Theta + t + s) \dot{\Delta}(s) \rangle = \frac{1}{\Theta} \int_{-\Theta}^0 dt \int_{-t}^0 ds \langle \dot{\Delta}(\Theta + t) \dot{\Delta}(0) \rangle \quad (\text{B5})$$

$$= \frac{1}{\Theta} \int_{-\Theta}^0 dt (\Theta + t) \langle \dot{\Delta}(\Theta + t) \dot{\Delta}(0) \rangle \quad (\text{B6})$$

$$= \frac{1}{\Theta} \int_0^\Theta dx x \langle \dot{\Delta}(x) \dot{\Delta}(0) \rangle. \quad (\text{B7})$$

A finite relaxation time τ means that $\langle \dot{\Delta}(t) \dot{\Delta}(0) \rangle \propto \exp(-t/\tau)$, which means that the last integral is finite for any finite τ . This is the case at T_c whenever the system size is finite since $\tau \propto L^z$. Consequently, the third term vanished in the limit $\Theta \rightarrow \infty$ for any finite L and the step from Eq. (29) to Eq. (30) follows.

¹ V. L. Berezinskii, Zh. Eksp. Teor. Fiz. **61**, 1144 (1972) [Sov. Phys. JETP **34**, 610 (1972)]; J. M. Kosterlitz and D. J. Thouless, J. Phys. C **6**, 1181 (1973); J. M. Kosterlitz, *ibid.* **7**, 1046 (1974).

² P. Minnhagen, Rev. Mod. Phys. **59**, 1001 (1987).

³ L. Onsager, Nuovo Cimento **6**, 249 (1949); R. Feynman, in *Progress in Low Temperature Physics*, edited by C. Gorter (North-Holland, Amsterdam, 1955), Vol. 1; G. A. Williams, Phys. Rev. Lett. **59**, 1926 (1987); **71**, 392 (1993); J. Low Temp. Phys. **93**, 1079 (1993); S. R. Shenoy, Phys. Rev. B **40**, 5056 (1989); P. Olsson and P. Minnhagen, *ibid.* **44**, 4503 (1991); B. Chattopadhyay, M. Mahato, and S. Shenoy, *ibid.* **47**, 15 159 (1993).

⁴ P. Minnhagen, in *Models and Phenomenology for Conventional and High-Temperature Superconductivity*, Proceedings of the International School of Physics ‘‘Enrico Fermi’’ Course CXXXVI, Varenna, 1997, edited by G. Iadonisi, J. R. Schrieffer, and M. L. Chiofalo (IOS Press, Amsterdam, 1998), p. 451.

⁵ H. Eikman and J. E. van Himbergen, Phys. Rev. B **41**, 8927 (1990).

⁶ J. J. Vicente Alvarez, D. Domínguez, and C. A. Balseiro, Phys. Rev. Lett. **79**, 1373 (1997); D. Domínguez, *ibid.* **82**, 181 (1999).

⁷ P. Olsson, Phys. Rev. B **46**, 14 598 (1992); **52**, 4511 (1995); **52**, 4526 (1995); Ph.D. thesis, Umeå University, 1992.

⁸ B. J. Kim, P. Minnhagen, and P. Olsson, Phys. Rev. B **59**, 11 506 (1999).

⁹ J. M. Kosterlitz and N. Akino, Phys. Rev. Lett. **82**, 4094 (1999); **81** 4672 (1998).

¹⁰ S. R. Shenoy, J. Phys. C **18**, 5163 (1985).

¹¹ P. C. Hohenberg and B. I. Halperin, Rev. Mod. Phys. **49**, 435 (1977).

¹² See, e.g., G. G. Batrouni, G. R. Katz, A. S. Kronfeld, G. P. Lepage, B. Svetitsky, and K. G. Wilson, Phys. Rev. D **32**, 2736 (1985) and references therein.

¹³ D. S. Fisher, M. P. A. Fisher, and D. A. Huse, Phys. Rev. B **43**, 130 (1991).

¹⁴ A. T. Dorsey, Phys. Rev. B **43**, 7575 (1991).

¹⁵ R. A. Wickham and A. T. Dorsey, Phys. Rev. B **61**, 6945 (2000).

¹⁶ J. Houlrik, A. Jonsson, and P. Minnhagen, Phys. Rev. B **50**, 3953 (1994).

¹⁷ F. Reif, *Fundamentals of Statistical and Thermal Physics* (McGraw-Hill, New York, 1965).

¹⁸ E. Granato, Phys. Rev. B **58**, 11 161 (1998).

¹⁹ H. Weber and H. J. Jensen, Phys. Rev. Lett. **78**, 2620 (1997).

²⁰ Z. B. Li, L. Schülke, and B. Zheng, Phys. Rev. Lett. **74**, 3396 (1995).

²¹ H. J. Luo and B. Zheng, Mod. Phys. Lett. B **11**, 615 (1997).

²² M. S. Soares, J. K. L. da Silva, and F. C. S. Barreto, Phys. Rev. B **55**, 1021 (1997).

²³ V. Ambegaokar, B. I. Halperin, D. R. Nelson, and E. D. Siggia, Phys. Rev. Lett. **40**, 783 (1978); Phys. Rev. B **21**, 1806 (1980); V. Ambegaokar and S. Teitel, *ibid.* **19**, 1667 (1979).

²⁴ P. Minnhagen, O. Westman, A. Jonsson, and P. Olsson, Phys. Rev. Lett. **74**, 3672 (1995).

²⁵ M. V. Simkin and J. M. Kosterlitz, Phys. Rev. B **55**, 11 646 (1997).

²⁶ K. Holmlund and P. Minnhagen, Phys. Rev. B **54**, 523 (1996); Physica C **292**, 255 (1997).

²⁷ M. Y. Choi, M. Yoon, and G. S. Jeon (unpublished).

²⁸ P. H. E. Tiesinga, T. J. Hagenaars, J. E. van Himbergen,

and J. V. José, Phys. Rev. Lett. **78**, 519 (1997).

²⁹ S. M. Ammirata, M. Friesen, S. W. Pierson, L. A. Gorham, J. C. Hunnicutt, M. L. Trawick, and C. D. Keener, Physica C **313**, 225 (1999); S. W. Pierson, M. Friesen, S. M. Ammirata, J. C. Hunnicutt, and L. A. Gorham, Phys. Rev. B **60**, 1309 (1999).

³⁰ D. Bormann, H. Beck, O. Gallus, and M. Capezzali, condmat/9910211 (unpublished).

³¹ In 2D, the XY model has $T_c \approx 0.892$, while in 3D $T_c \approx 2.2018$ with the static exponent $\nu \approx 0.6720$, P. Olsson (unpublished).

³² A. Jonsson and P. Minnhagen, Phys. Rev. B **55**, 9035 (1997).

³³ V. Pasler, P. Schweiss, C. Meingast, B. Obst, H. Wühl, A. I. Rykov, and S. Tajima, Phys. Rev. Lett **81**, 1094 (1998).

³⁴ A. Pomar, A. Diaz, M. V. Ramallo, C. Torrón, J. A. Veira, and F. Vidal, Physica C **218**, 257 (1993); W. Holm, Y. Eltsev, and Ö. Rapp, Phys. Rev. B **51**, 11 992 (1995).

³⁵ J. C. Booth, D. H. Wu, S. B. Qadri, E. F. Skelton, M. S. Osofsky, A. Pique, and S. M. Anlage, Phys. Rev. Lett. **77**, 4438 (1996); J.-T. Kim, N. Goldenfeld, J. Giapintzakis, and M. Ginsberg, Phys. Rev. B **56**, 118 (1997).

³⁶ K. Moloni, M. Friesen, S. Li, V. Souw, P. Metcalf, L. Hou, and M. McElfresh, Phys. Rev. Lett. **78**, 3173 (1997).

³⁷ J.-T. Kim, S. H. Chung, D. H. Ha, K. H. Yoo, Y. K. Park, J. C. Park, M. S. Kim, and S. I. Lee, IEEE Trans. Magn. **MAG-35**, 4082 (1999).

³⁸ S. Ryu and D. Stroud, Phys. Rev. B **57**, 14 476 (1998).

³⁹ J. Lidmar, M. Wallin, C. Wengel, S. M. Girvin, and A. P. Young, Phys. Rev. B **58**, 2827 (1998).

⁴⁰ L. M. Jensen, B. J. Kim, and P. Minnhagen, Europhys. Lett. **49**, 644 (2000).

⁴¹ P. Olsson (private communication).

⁴² Preliminary results for the 4D XY model can be found in L. M. Jensen, B. J. Kim, and P. Minnhagen, Physica B **284**, 455 (2000).

⁴³ K. Binder and D. W. Heermann, *Monte Carlo Simulation in Statistical Physics*, 2nd ed. (Springer-Verlag, Berlin, 1992).

⁴⁴ A. K. Bukenov, U.-J. Wiese, M. I. Polikarpov, and A. V. Pochinskii, Yad. Fiz. **56**, 214 (1993) [Phys. At. Nucl. **56**, 122 (1993)].

⁴⁵ N. Goldenfeld, *Lectures on Phase Transitions and the Renormalization Group* (Addison-Wesley, Reading, MA, 1992).

⁴⁶ H. Weber, M. Wallin, and H. J. Jensen, Phys. Rev. B **53**, 8566 (1996).

⁴⁷ D. R. Nelson and J. M. Kosterlitz, Phys. Rev. Lett. **39**, 1201 (1977).

⁴⁸ P. Minnhagen and G. G. Warren, Phys. Rev. B **24**, 2526 (1981).

⁴⁹ For RSJD at $T = 1.40$ with $L = 64$, $R \approx 0.44$ and $R \approx 0.425$ were obtained for the FTBC and PBC, respectively.

⁵⁰ Model F gives $z = 3/2$ in 3D when the specific heat exponent is less or equal to zero, which is the case for the 3D XY model.

⁵¹ Explicitly checked and confirmed in 2D (see Ref. 49), but should apply also in 3D.

⁵² K. H. Lee and D. Stroud, Phys. Rev. B **46**, 5699 (1992).

⁵³ M. Krech and D. P. Landau, Phys. rev. B **60**, 3375 (1999).

⁵⁴ The validity of using the 3D XY model to describe high- T_c superconductors is still under debate. See, e.g., M. Charalambous, O. Riou, P. Gandit, B. Billon, P. Lejay, J. Chaussy, W. N. Hardy, D. A. Bonn, and R. Liang, Phys. Rev. Lett. **83**, 2042 (1999); A. Junod, A. Erb, and C. Renner, Physica C **317-318**, 333 (1999).

⁵⁵ J.-T. Kim, Y. K. Park, J.-C. Park, H. R. Lim, S. Y. Shim, D. H. Kim, W. N. Kang, J. H. Park, T. S. Hanh, S. S. Choi, W. C. Lee, J. D. Hettinger, and K. E. Gray, Phys. Rev. B **57**, 7499 (1998).

⁵⁶ It is shown that the initial configuration can change the short-time relaxation z in A. J. Bray, A. J. Briant, and D. K. Jervis, Phys. Rev. Lett. **84**, 1503 (2000).

⁵⁷ H. Weber and P. Minnhagen, Phys. Rev. B **37**, 5986 (1988).

TABLE I. Dynamic critical exponent z for 2D RSJD and RD with the PBC and FTBC.

	RSJD		RD	
	PBC	FTBC	PBC	FTBC
at $T = 0.90$				
resistance scaling	–	2.0(1)	–	2.0(1)
supercurrent scaling	1.5(1)	–	2.0(1)	–
short-time relaxation	1.2(1)	2.0(1)	2.0(1)	2.0(1)
at $T = 0.80$				
resistance scaling	–	3.3(1)	–	3.3(1)
short-time relaxation	1.4(1)	3.2(1)	2.0(1)	2.0(1)
above T_c				
from $\omega_0 \sim \xi^{-z}$	~ 2	–	2.0 ^a	–

^a Reference 32

TABLE II. Dynamic critical exponent z for 3D RSJD and RD with the PBC and FTBC.

	RSJD		RD	
	PBC	FTBC	PBC	FTBC
resistance scaling	–	1.46(6)	–	1.5(1)
supercurrent scaling (L)	1.5(1)	–	2.0(1)	–
supercurrent scaling (ξ)	1.4(1)	–	1.9(2)	–
short-time relaxation	1.2(1)	1.50(5)	2.1(1)	2.0(1)

TABLE III. Dynamic critical exponent z for 4D RSJD and RD both with the FTBC.

	RSJD	RD
resistance scaling	~ 2	~ 2
short-time relaxation	2.0(1)	2.0(1)

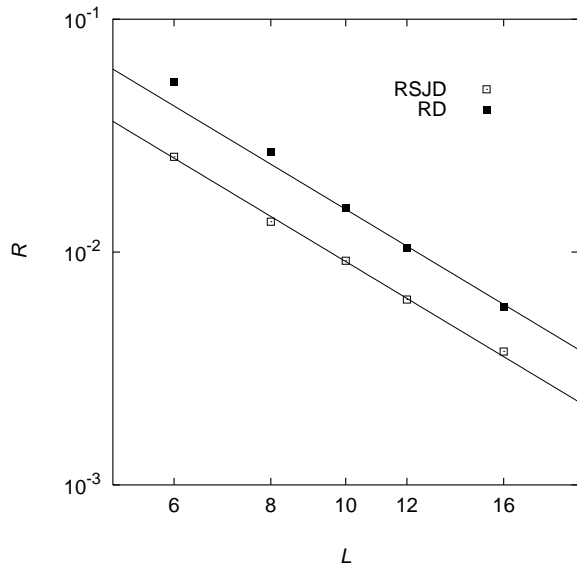


FIG. 1. Resistance scaling for 2D RSJD (open squares) and RD (solid squares) with the FTBC at $T=0.9$. The solid lines represent $R \sim L^{-2.0}$. For both dynamics, $z \approx 2.0$ is obtained. (The data points were taken from Ref. 8.)

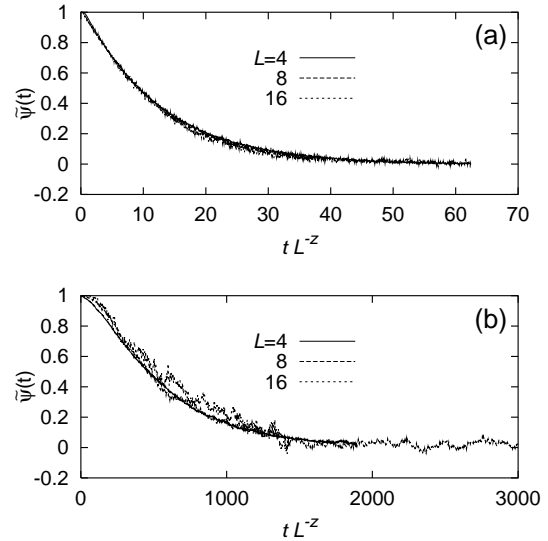


FIG. 3. Short-time relaxation for 2D RSJD at $T = 0.9$. (a) For the FTBC $z \approx 2.0$ and (b) for the PBC $z \approx 1.2$ are obtained. Note the enormous time scale for the PBC.

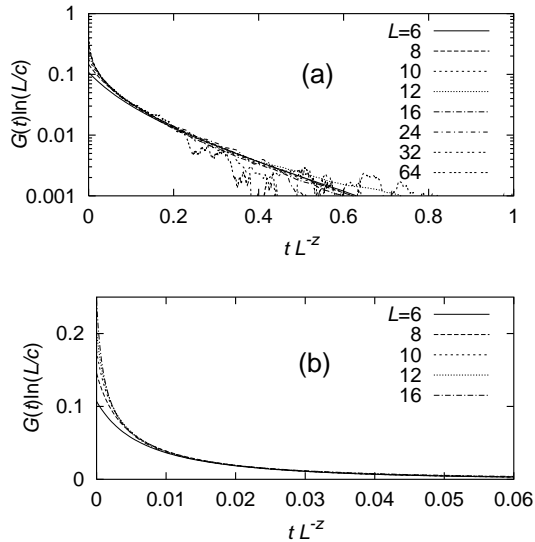


FIG. 2. Scaling of the supercurrent correlation function $G(t)$ in 2D at the KT transition ($T = 0.9$) in case of the PBC for (a) RSJD and (b) RD. The scaling collapse of the data shown is for $z = 1.5$ and 2.0 in case of (a) RSJD and (b) RD, respectively. [The apparent spread of the data in (a) is only due to the logarithmic scale and insufficient convergence for the largest lattice sizes at large t .]

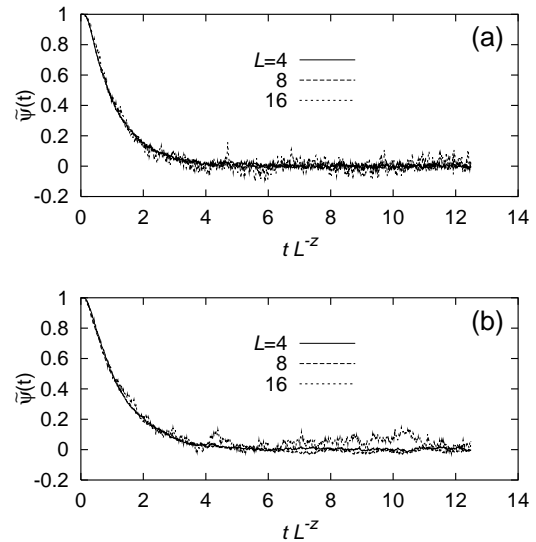


FIG. 4. Short-time relaxation for 2D RD at $T = 0.9$ with the (a) FTBC and (b) PBC. For both boundary conditions $z \approx 2.0$ is obtained from the data collapse. Note that the decays for both boundary conditions have the same time scale.

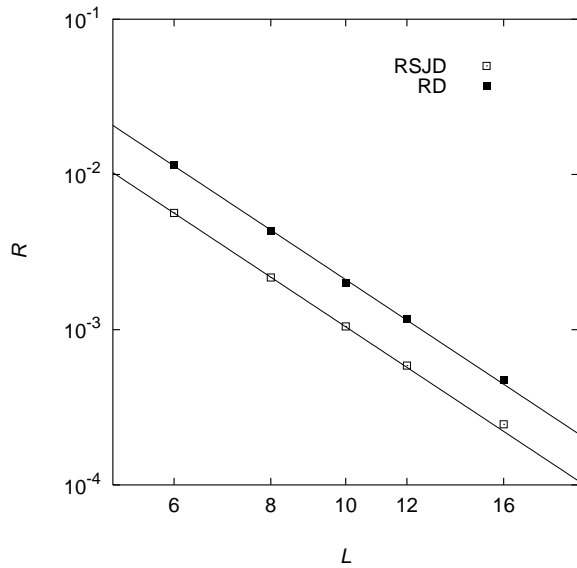


FIG. 5. Resistance scaling for 2D RSJD (open squares) and RD (solid squares) with the FTBC at $T=0.8$. For both dynamics, $z \approx 3.3$ is obtained from the slopes of the lines in the figure. (The data points were taken from Ref. 8.)

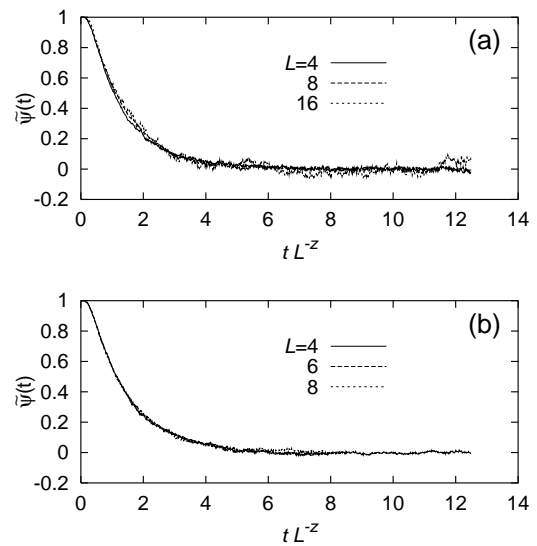


FIG. 7. Short-time relaxation for 2D RD at $T = 0.80$ for the (a) FTBC and (b) PBC. For both boundary conditions, $z \approx 2.0$ is found from the best data collapse.

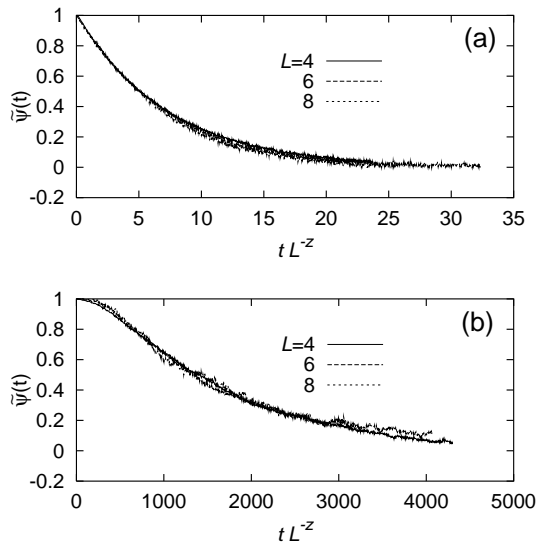


FIG. 6. Short-time relaxation for 2D RSJD at $T = 0.80$. (a) For the FTBC $z \approx 3.2$ and (b) for the PBC $z \approx 1.4$ are obtained from the best data collapse.

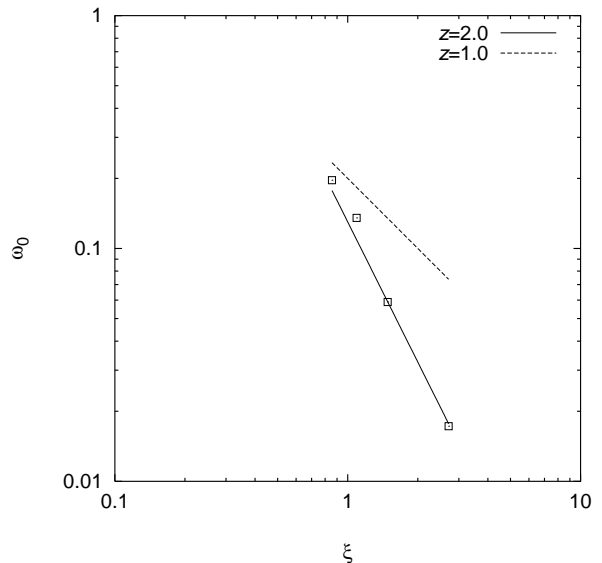


FIG. 8. Characteristic frequency ω_0 determined from the peak position of $|\text{Im}1/\epsilon(\omega)|$ vs the correlation length ξ for 2D RSJD with the PBC at temperatures $T = 1.0, 1.1, 1.2$, and 1.3 (from right to left). The dynamic critical exponent z defined by $\omega_0 \sim \xi^{-z}$ is shown to have a value close to 2.0 (solid line). For comparison, we also plot the dotted line which corresponds to $z = 1.0$.

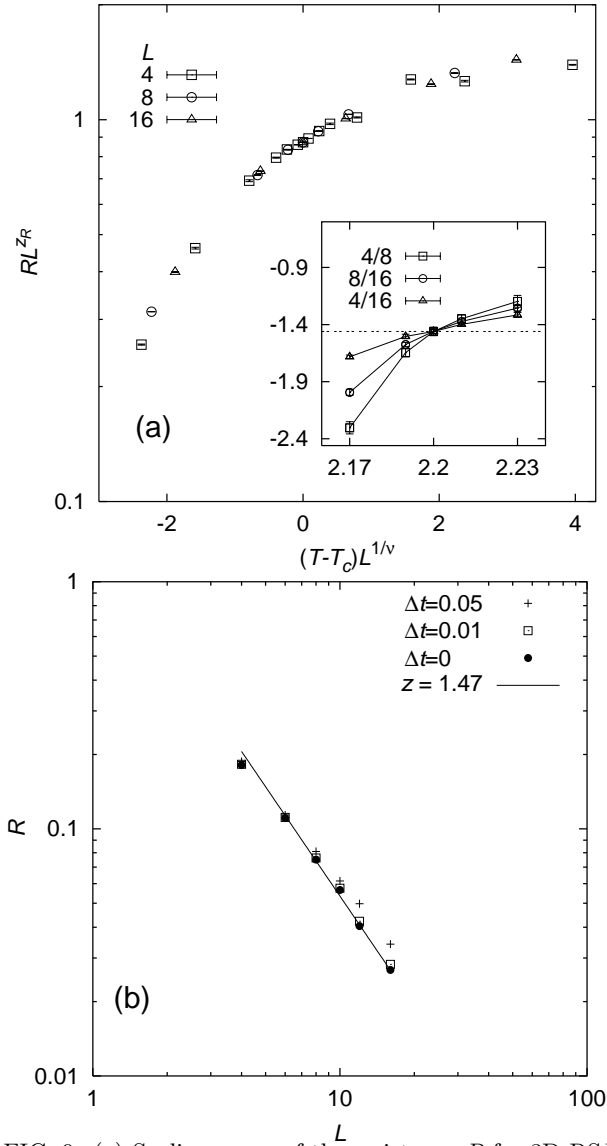


FIG. 9. (a) Scaling curve of the resistance R for 3D RSJD with the FTBC for $L = 4, 8,$ and 16 at $T = 2.17, 2.19, 2.20, 2.21,$ and 2.23 with parameter values $z = 1.46$ and $T_c = 2.200$ (both from the intersection method described in the text and shown in the inset), and the known value $\nu = 0.67$ (Ref. 31). (b) Determination of z for 3D RD with the FTBC from the resistance scaling form $R \propto L^{-z}$ at $T_c = 2.20$. The data points are for $L = 4, 8, 10, 12,$ and 16 , and two integration time steps $\Delta t = 0.05$ and 0.01 . Linear extrapolation to $\Delta t = 0$ gives $z = 1.47$ from the least-squares fit.

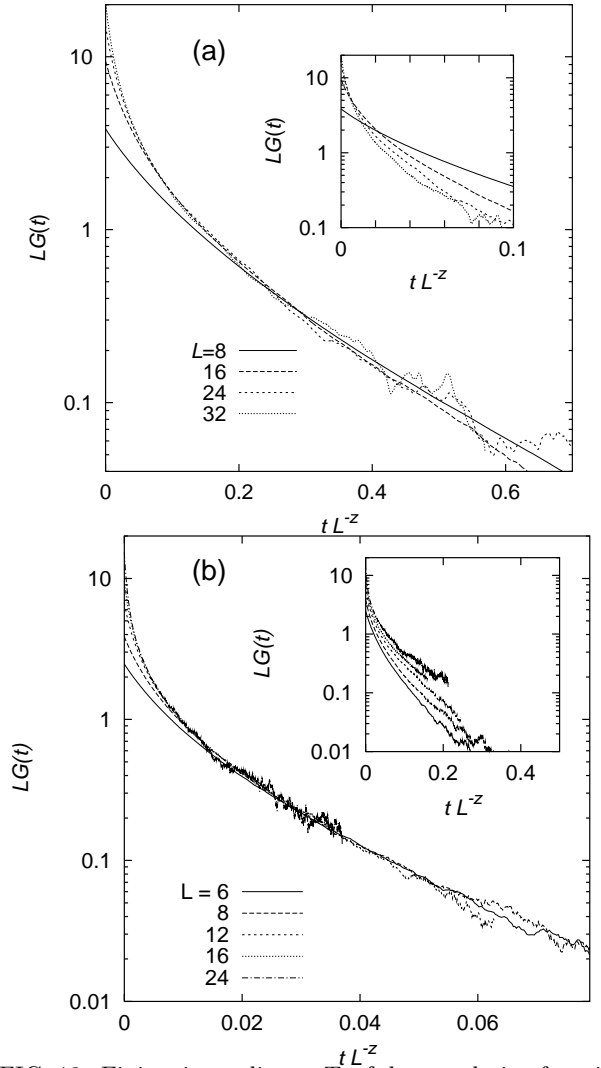


FIG. 10. Finite-size scaling at T_c of the correlation function $LG(t)$ vs t/L^z for 3D (a) RSJD with the PBC and (b) RD with the PBC. In the main parts of (a) and (b), $z = 1.5$ and $z = 2.05$ are shown to give good scaling collapses for (a) RSJD and (b) RD, respectively, while in the insets the interchanged values [$z = 2.0$ and $z = 1.5$ for (a) and (b), respectively] are shown to be inconsistent with the scaling collapse.

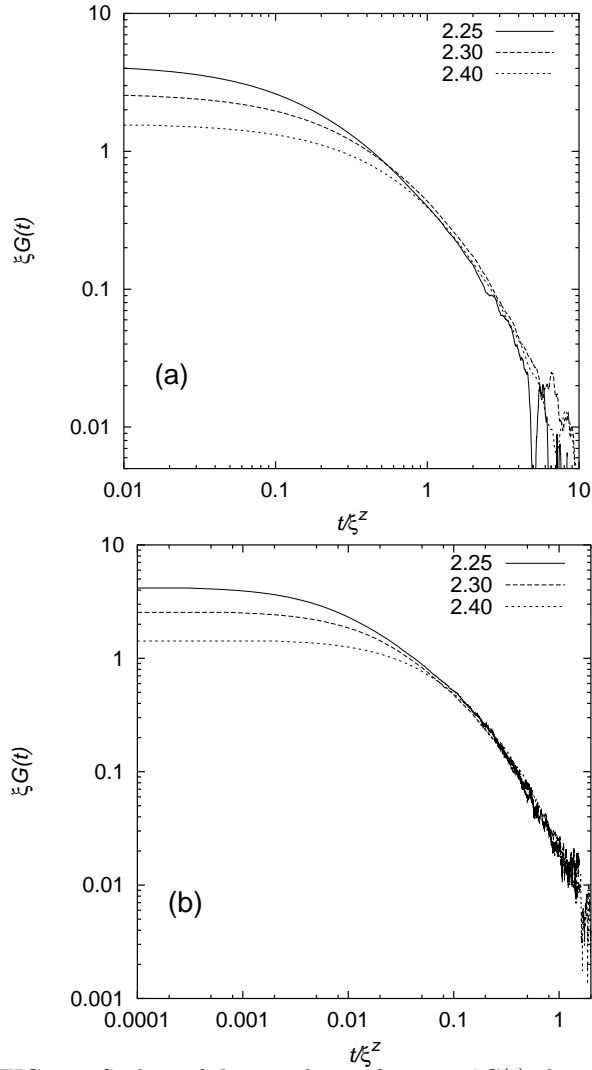


FIG. 11. Scaling of the correlation function $\xi G(t)$ above T_c is shown against the scaling variable $t\xi^z$ for 3D (a) RSJD with the PBC and (b) RD with the PBC for $L = 24$ and $T = 2.25, 2.30,$ and 2.40 . From the scaling collapse, with ξ from the MC simulation (Ref. 41), we obtain (a) $z \approx 1.4$ for RSJD and (b) $z \approx 1.9$ for RD.

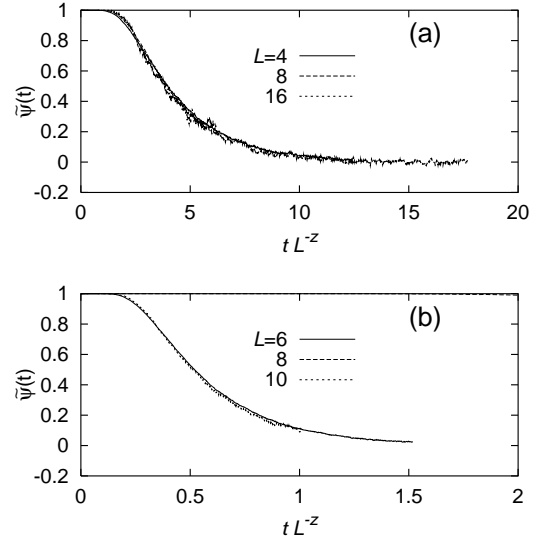


FIG. 12. Short-time relaxations of $\tilde{\psi}$ in 3D with the FTBC at $T = T_c = 2.20$ are shown as functions of the scaling variable tL^{-z} for (a) RSJD with $L = 4, 6,$ and 16 , and for (b) RD with $L = 6, 8,$ and 10 . From the scaling collapse $z = 1.50$ and $z = 1.95$ are found to yield smoothly collapsed single curves for (a) RSJD and (b) RD, respectively.

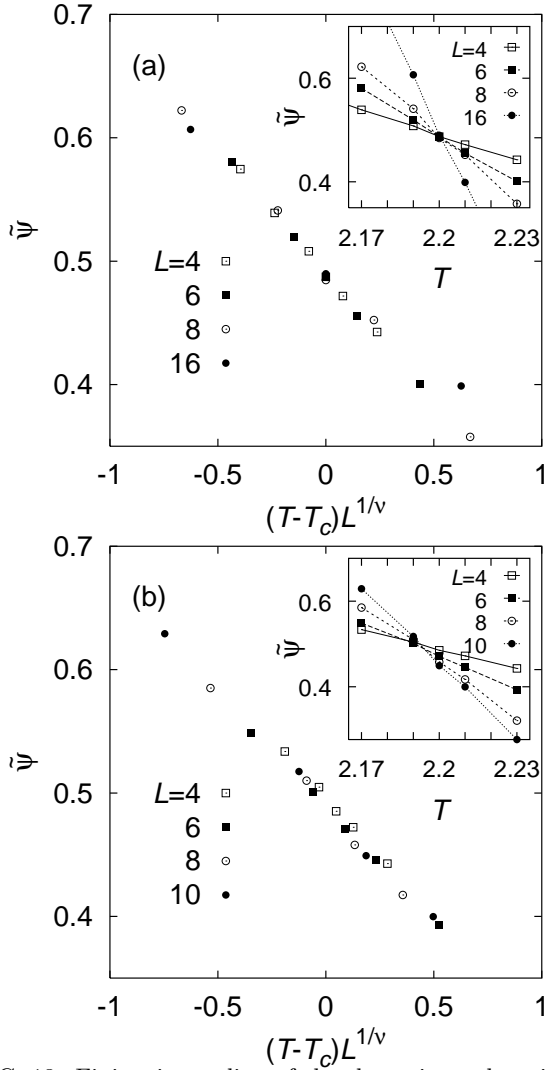


FIG. 13. Finite-size scaling of the short-time relaxation of $\tilde{\psi}$ for 3D (a) RSJD for $L = 4, 6, 8,$ and 16 and (b) RD for $L = 4, 6, 8,$ and 10 both with the FTBC and at $T = 2.17, 2.19, 2.20, 2.21,$ and 2.23 . As shown in insets, the scaling function $\tilde{\psi} = F_{\tilde{\psi}}(t/L^z, (T - T_c)L^{1/\nu})$ with a fixed $a = t/L^z$ suggests the existence of a single crossing point (a) at $T_c = 2.200$ with $(z, a) = (1.5, 4.0)$ for RSJD and (b) at $T_c = 2.194$ with $(z, a) = (2.0, 0.5)$ for RD. All data points in the insets collapse onto a single smooth curve with the scaling variable $(T - T_c)L^{1/\nu}$ for both models with the known value $\nu = 0.67$ (Ref.³¹), as shown in main parts.

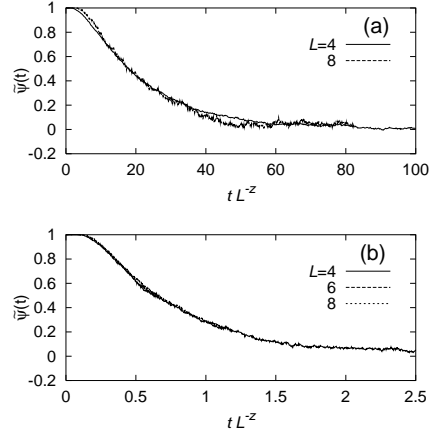


FIG. 14. Short-time relaxation of $\tilde{\psi}$ in 3D with the PBC at $T = T_c = 2.20$ as functions of the scaling variable tL^{-z} for (a) RSJD with $L = 4$ and 8 , and for (b) RD with $L = 4, 6,$ and 8 . From the scaling collapse $z \approx 1.2$ and $z \approx 2.1$ are found for (a) RSJD and (b) RD, respectively.

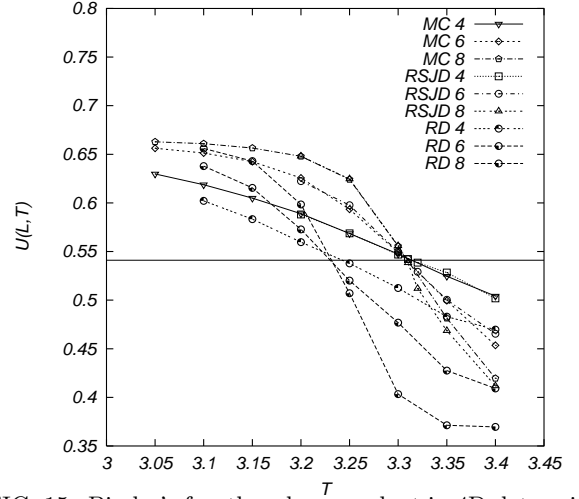


FIG. 15. Binder's fourth order cumulant in 4D determined from MC simulations, RSJD, and RD for $L = 4, 6,$ and 8 at several temperatures between $T = 3.05$ and $T = 3.40$. Data points for MC and RSJD coincide within error bars and give $T_c \approx 3.31$, whereas the RD results show a relative large dynamic shift to $T_c \approx 3.25$.

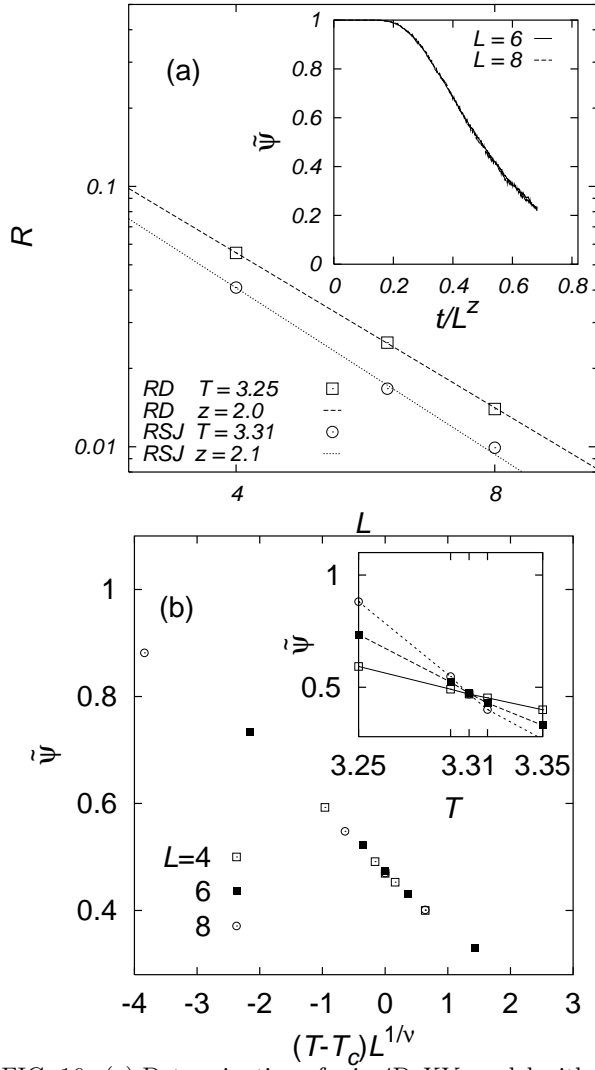


FIG. 16. (a) Determination of z in 4D XY model with the FTBC from the resistance scaling form $R \sim L^{-z}$ for $L = 4, 6,$ and 8 at $T_c = 3.31$ for RSJD and at $T_c = 3.25$ for RD (see Fig. 15). From the slopes in log-log plot, $z \approx 2$ is concluded for both dynamics. Inset: Short-time relaxation of $\tilde{\psi}$ for 4D RD with the FTBC at $T = T_c = 3.25$ is shown against the scaling variable tL^{-z} for $L = 6$ and 8 and $z = 2.0$ is found. (b) Finite-size scaling of $\tilde{\psi}$ for 4D RSJD with the FTBC for $L = 4, 6,$ and 8 at $T = 3.25, 3.30, 3.31, 3.32,$ and 3.35 . As shown in inset, the intersection method gives $T_c \approx 3.31$ with $z = 2.0$. The main part displays the full scaling plot of the form $\tilde{\psi} = F_{\tilde{\psi}}(t/L^z, (T-T_c)L^{1/\nu})$ with $a = tL^z = 2.8$ and the mean-field value $\nu = 1/2$.